



Cooperative Research Centre for  
Landscape Environments  
and Mineral Exploration



OPEN FILE  
REPORT  
SERIES

# THE MINERALOGY AND GEOCHEMISTRY OF NEW COBAR Au-Cu MINERALISATION IN THE OXIDATE AND SUPERGENE ZONES, COBAR DISTRICT, WESTERN NSW

*K. M. Scott and K. G. McQueen*

**CRC LEME OPEN FILE REPORT 213**

**February 2008**

CRCLEME

(CRC LEME Restricted Report I67R /  
CSIRO Exploration and Mining Report 845R, 2001  
2nd Impression 2008)

CRC LEME is an unincorporated joint venture between CSIRO-Exploration & Mining, and Land & Water, The Australian National University, Curtin University of Technology, University of Adelaide, Geoscience Australia, Primary Industries and Resources SA, NSW Department of Primary Industries and Minerals Council of Australia, established and supported under the Australian Government's Cooperative Research Centres Program.





# **THE MINERALOGY AND GEOCHEMISTRY OF NEW COBAR Au-Cu MINERALISATION IN THE OXIDATE AND SUPERGENE ZONES, COBAR DISTRICT, WESTERN NSW**

*K. M. Scott and K. G. McQueen*

**CRC LEME OPEN FILE REPORT 213**

February 2008

(CRC LEME Restricted Report 167R /  
CSIRO Exploration and Mining Report 845R, 2001  
2nd Impression 2008)

© CRC LEME 2008

---

CRC LEME is an unincorporated joint venture between CSIRO-Exploration & Mining, and Land & Water, The Australian National University, Curtin University of Technology, University of Adelaide, Geoscience Australia, Primary Industries and Resources SA, NSW Department of Primary Industries and Minerals Council of Australia.

*Headquarters:* CRC LEME c/o CSIRO Exploration and Mining, PO Box 1130, Bentley WA 6102, Australia

Open File Report 213 is a second impression (second printing) of CRC for Landscape Evolution and Mineral Exploration Restricted Report 167R. It was produced in July 2001 for Peak Gold Mines Pty Ltd. The period of Confidentiality has now expired. Thanks and acknowledgements are extended to Peak Gold Mines Pty Ltd.

Electronic copies of this publication in PDF format can be downloaded from the CRC LEME website: <http://crcleme.org.au/Pubs/OFRSindex.html>. Information on this and other LEME publications can be obtained from <http://crcleme.org.au>.

Hard copies will be retained in the Australian National Library, the Western Australian State Reference Library, and Libraries at The Australian National University and Geoscience Australia, Canberra, The University of Adelaide, and the CSIRO Library at the Australian Resources Research Centre, Kensington, Western Australia.

**Reference:**

Scott KM and McQueen KG. 2008. The mineralogy and geochemistry of New Cobar Au-Cu mineralisation in the oxidate and supergene zones, Cobar District, western NSW. *CRC LEME Open File Report 213*. 18pp plus Appendices and Figures.

**Keywords:**

1. Mineralogy. 2. Mineralisation. 3. Geochemistry. 4. Gold. 5. Copper. 6. Supergene zones. 7. Oxidate 8. Cobar, New South Wales

ISSB 1329-4768

ISBN 1 921039 58 2

**Addresses and affiliations of authors**

**Mr Keith Scott**

Honorary Research Fellow, CRC LEME  
CSIRO Exploration and Mining  
PO Box 136  
North Ryde NSW 2113

**Assoc Prof Ken McQueen**

Honorary research Fellow, CRC LEME  
Division of Science and Design  
University of Canberra  
Canberra ACT 2601

**Published by:**

CRC Landscape Environments and Mineral Exploration,  
c/o CSIRO Exploration and Mining  
PO Box 1130  
Bentley, Western Australia 6102

**Disclaimer**

The user accepts all risks and responsibility for losses, damages, costs and other consequences resulting directly or indirectly from using any information or material contained in this report. To the maximum permitted by law, CRC LEME excludes all liability to any person arising directly or indirectly from using any information or material contained in this report.

© **This report is Copyright of the** Cooperative Research Centre for Landscape Evolution and Mineral Exploration, (2001), which resides with its Core Participants: CSIRO Exploration and Mining, University of Canberra, The Australian National University and Geoscience Australia (formerly Australian Geological Survey Organisation).

Apart from any fair dealing for the purposes of private study, research, criticism or review, as permitted under Copyright Act, no part may be reproduced or reused by any process whatsoever, without prior written approval from the Core Participants mentioned above.

## TABLE OF CONTENTS

<b>SUMMARY</b>	<b>1</b>
<b>1. Introduction</b>	<b>2</b>
<b>2. Geology</b>	<b>2</b>
<b>3. Mineralisation</b>	<b>3</b>
<b>4. Samples and Methods</b>	<b>3</b>
<b>5. Results</b>	<b>4</b>
5.1 DD97NC0054 and RC00CA0602	4
5.2 DD97NC0059	4
5.3 DD97NC0060	7
<b>6. Discussion</b>	<b>10</b>
6.1 Weathering of the New Cobar ore	10
6.2 Mineralogical variations in the regolith profile	12
<b>7. Conclusions and Recommendations</b>	<b>13</b>
<b>8. Acknowledgements</b>	<b>14</b>
<b>9. References</b>	<b>15</b>

## LIST OF TABLES

<b>Table 1. Average composition of intervals in drill holes DD97NC0054 and RC00CA0602, New Cobar (ppm, unless otherwise indicated)</b>	<b>5</b>
<b>Table 2. Average composition of intervals in drill hole DD97NC0059, New Cobar (ppm, unless otherwise indicated)</b>	<b>6</b>
<b>Table 3. Average compositions of intervals in drill hole DD97NC0060, New Cobar (ppm, unless otherwise indicated)</b>	<b>8</b>
<b>Table 4. Average Minor and Trace Element contents in Goethite and hematite, New Cobar (ppm, unless otherwise indicated) – determined by electron microprobe.</b>	<b>9</b>
<b>Table 5. Average compositions of Mn oxide phases, New Cobar (wt%) – determined by electron microprobe</b>	<b>10</b>
<b>Table 6. Average composition of ore at various depths in the profile at New Cobar (from Tables 1-3 and Scott and McQueen, 2000: ppm, unless otherwise indicated)</b>	<b>11</b>

## LIST OF APPENDICES

<b>Appendix 1 Sample descriptions, New Cobar - DD97NC054</b>	<b>16</b>
<b>Appendix 2 Composition of samples, DD97NC0054 and RC00CA0602, New Cobar (ppm, unless indicated otherwise)</b>	<b>19</b>
<b>Appendix 3 Composition of samples, DD97NC0059, New Cobar (ppm, unless indicated otherwise)</b>	<b>21</b>
<b>Appendix 4 Composition of samples, DD97NC0060, New Cobar (ppm, unless indicated otherwise)</b>	<b>24</b>

## LIST OF FIGURES

- Figure 1.** The location of the New Cobar Deposit in the Cobar Gold Field (after Stegman and Pocock, 1996; Leah and Roberts, 2000)
- Figure 2.** Location of drill holes and profiles at the New Cobar South Open Pit
- Figure 3.** Section at 16025N, New Cobar (after Peak Gold Mines Pty Ltd)
- Figure 4.** Mineralogical variation below the base of complete oxidation in DD97NC0060, New Cobar (determined by X-ray Diffraction)
- Figure 5.** Compositional variations in cryptomelane-hollandite-coronadite series minerals, New Cobar
- Figure 6.** Section at 16025 N, New Cobar, showing the distribution of sulfides, pyrite casts and gossanous features
- Figure 7.** Section at 16025 N, New Cobar, showing the distribution of dominant kaolinite and muscovite
- Figure 8.** Section at 16025 N, New Cobar, showing the distribution of zones of silicification and abundant quartz veining
- Figure 9.** Section at 16025 N, New Cobar, showing the distribution of abundant Mn
- Figure 10.** Schematic summary of some major and minor element hosts in the primary and oxidised zones, New Cobar
- Figure 11.** Location of drill holes and profiles at the New Cobar South Open Pit, showing Pb content (ppm) in near surface samples

## SUMMARY

Study of oxidised and supergene Cu-Au mineralisation at New Cobar, provided by integrating results from 164 drill hole samples with data previously obtained from the open pit study (Scott and McQueen, 2000), has revealed the nature of the dispersion of Au and its pathfinder elements. Weathering occurred at two different stages:- initially under acidic sulfate conditions to form secondary sulfides, sulfates, alunite-jarosite minerals and Fe- and Mn- oxides in a mature gossan profile and then under more arid conditions. This latter period, when Cl-rich fluids overprinted pre-existing minerals, is also believed to be largely responsible for the loss of Ag relative to Au up to about 40 m depth and then loss of Au in the top 15 m of the gossanous profile. Some elements, like Zn and Cd, are strongly depleted as soon as the sulfides commenced weathering and others, like Mo and W, appear to be concentrated at about 100-110 m depth in the supergene sulfide zone and Se at 30-40 m depth within the gossanous Fe oxides. Copper contents vary more systematically up the profile but even in this case abundance drop by almost an order of magnitude above 65 m.

Examination of the Pb contents in near-surface samples suggests that elevated Pb (>300 ppm) may occur up to 70 m south from the mineralisation. The presence of an extensive Pb anomaly about the economic mineralisation may be useful during surficial regional exploration.

## 1. Introduction

The Cobar Gold Field, near Cobar in western New South Wales, has produced over 2 million ounces of Au since the 1870's (Stegman, 2000) with a substantial proportion coming from oxidised ore. With the commencement of open cut mining at the New Cobar mine (145° 51'E, 31° 31'S), 2 km south of Cobar township, during 1998, Scott and McQueen (2000) were able to study the effects of weathering of Au-Cu mineralisation in the top 30 m of the regolith as exposed by that mining. They found that Au mineralisation at the deposit is associated with Ag, As, Bi, Cu, Mo, Pb, Sb, Se and W in the outcropping sub-vertical lode material. Sub-horizontal veins are also strongly mineralised for up to 6 m from the sub-vertical lodes with anomalous Au, Ag, Pb and Cu extending out for at least another 25 m. Thus, a lateral progression from Au-Ag-Pb-Cu to those elements, *plus* Bi, Mo, Se (and perhaps Sb and W), would be expected as mineralisation is approached.

In the mineralised profile, Au was separated from Ag during weathering to form pure supergene gold. There is no evidence of supergene enrichment of Au and, in fact, there appears to be substantial depletion of Au close to the surface. Thus, use of the Au pathfinders in near-surface sampling during regional exploration was strongly recommended. They also suggested that documentation of the material below 30 m by using drill core samples before renewed mining reached the deeper material might be helpful.

This study specifically addresses the behaviour of potential pathfinder elements including Ag, As, Bi, Sb, W and Zn as well as Au and Cu to better understand element movements during weathering and to make suggestions on how that knowledge may be used in on-going exploration in the Cobar region. Documentation of variations in the regolith profile also provide information of likely benefit in understanding the behaviour of oxide ore during metallurgical processing.

## 2. Geology

The New Cobar deposit occurs about midway along the 10 km long north-trending Cobar Gold Field (Figure 1). All the deposits in the goldfield are structurally controlled and located near the eastern margin of the early Devonian Cobar Basin (Glen, 1991). The New Cobar deposit occurs within siltstones and sandstones of the Great Cobar Slate, immediately west of a thrust contact (Great Chesney Fault) with the more arenaceous Chesney Formation. The mineralisation occurs adjacent to a pronounced bend in the thrust. At its northern end, mineralisation is only 20 m from the thrust but is up to 150 m from the thrust at its southern end. Movement along the Great Chesney Fault was complex and probably occurred over an extended period (Stegman and Pocock, 1996).

Since the Late Cretaceous, rocks of the Cobar region have been subjected to chemical weathering under both wet-humid and, more recently, arid conditions. Relative tectonic stability for most of this period allowed the development of thick weathering profiles that underwent variable erosional stripping, particularly during the Late Miocene (Leah, 1996). Thus, preserved profiles vary considerably from thin (<3 m) profiles over weakly weathered near-surface saprock or bedrock to thick (up to 100 m) intensely weathered *in situ* profiles. The latter are characterised by a red silty loam soil with surface ferruginous and lithic lag, overlying collapsed and ferruginised saprolite over bleached saprolite with variable ferruginous mottling above the water table. Older weathering profiles are commonly overprinted by the effects of later weathering under drier conditions marked by lower or fluctuating water table levels (Leah, 1996).

Silicification and ferruginisation associated with the mineralisation and its weathering at New Cobar has resulted in a positive surface expression of the deposit. The resulting hill has been subjected to erosional stripping for a long period and soils above the deposit are only a few centimetres thick. Although the area has been disturbed by 19<sup>th</sup> century mining activity, soils there were probably never thick due to the sustained erosion of the hill. Aeolian material has probably been added to the soil during the Quaternary.

### 3. Mineralisation

Although Au was recognised as a component of the Cu ores at Cobar, Au was not sought as a commodity in its own right until the late 1880's when the association of silicification and Au was recognised at Fort Bourke Hill *i.e.* the New Cobar area (Stegman and Stegman, 1996). The Au mineralisation at New Cobar occurs in four steeply east-dipping Au-Cu lenses in the Great Cobar Slate adjacent to a thrust contact with the Chesney Formation (see above). Paragenesis of the deposit is complex, with nine stages being recognised by Peak Gold Mines geologists (Leah and Roberts, 2000). Nevertheless it is clear that the economic mineralisation is present in the NW-trending sub-vertical quartz-breccia and base metal sulfide veins which occur within a broader envelope of disseminated pyrite. The Au occurs in three associations:– (i) most commonly as Ag-bearing Au with Bi minerals (along grain boundaries and as submicron inclusions), (ii) as generally Ag-poor, free Au along fractures and silicate grain boundaries and (iii) as Ag-rich Au associated with chalcopyrite (P.A. Leah, pers. comm., 1999).

Complete weathering at the deposit extends to about 60 m with partial oxidation extending another 40 m. The transition from primary ore to secondary mineralisation is marked by the appearance of supergene Cu minerals (native Cu and chalcocite) with Cu carbonates present where all of the sulfides, except pyrite, have oxidised. Weathering of the base metal sulfides has produced the Fe oxides and oxidate minerals of the alunite-jarosite group which dominate the profile to the surface. Gold is generally retained at similar levels to those in the primary ore up the profile, except in the top 10-15 m where it is strongly leached. There is no obvious zone of supergene Au enrichment (P.A. Leah, pers. comm., 2000).

### 4. Samples and Methods

After discussion with Peter Leah, a program of sampling from three diamond and two reverse circulation drill holes to provide samples of ore at various depths below the current open pit was devised (see Figure 2). A suite of 164 samples (about 10 cm long) was collected from these drill holes with the assistance of Peak Gold Mines personnel during November 2000. Brief sample descriptions are provided in Appendix 1. (Some of the samples were also used to illustrate textures/features in an atlas: McQueen *et al.*, 2001).

After examination, 76 samples from four drill holes were crushed to <75 µm using a Mn-steel mill. They were then analysed by Analabs (Perth) for Al, Mg, Ca, Ti, Mn, P, S, Cu, Ni, Pb, Sr, V, Zn, and Zr by inductively coupled plasma emission spectrometry (ICP) and for Ag, Bi, Cd, Cu and Mo by inductively coupled plasma emission mass spectrometry (ICP-MS) after a HF/HCl/HNO<sub>3</sub>/HClO<sub>4</sub> digestion. (It is recognised that possible incomplete dissolution of rutile and zircon means that the Ti and Zr values so obtained may represent minimum rather than “total” values for some samples.) Neutron activation analysis (NAA) for the “Au+31 suite” was also performed by Becquerel Laboratories (Lucas Heights) for each sample. Results are reported in Appendices 2-4. Although the NAA suite provided Ca, Ag, Mo and Zn



determinations, detection limits are high and only the determinations of Ca and Zn (by ICP) and Ag and Mo (by ICP-MS) are quoted in the appendices.

After receipt of the chemical analyses, 27 samples (mainly from DD97NC0060) were chosen as representative of specific stages of weathering and were analysed mineralogically by X-ray diffraction, using graphite-crystal monochromated, Cu radiation.

Seventy-seven Fe and Mn oxides in 6 samples were analysed by electron microprobe at the Research School of Earth Sciences, ANU. Major and minor elements were analysed using 40 second counting times allowing Co, Cu, Ni, S and Zn to be determined down to a detection limit ~140 ppm, and Pb to be determined above 1000 ppm. The composition of chalcocite, cuprite and sphalerite was also confirmed by electron microprobe analysis.

## 5. Results

### 5.1 DD97NC0054 and RC00CA0602

The analyses of samples from these two drill holes provide sections of the ore at depths of 20-40 m and 65-75 m below the surface at New Cobar respectively (Figure 3). Note that, because of the projection of the drill holes onto the 16025N section, grades from individual drill holes and outlines from the section do not correspond perfectly.

Comparison of material from the ore interval with slightly deeper peripheral material in DD97NC0054 indicates that the ore interval has substantially higher Ag, As, Au, Bi, Se and W but lower Al, Mg, Ca, Na, K, Ti, S, Cr, Mo, Th and V than the more peripheral material (Table 1). Despite relatively similar Au grades, the upper portion of this ore interval (20-30 m) tends to be depleted in Fe, Mn, P, S, As, Bi, Cu, Mo, Pb, Se and Zn relative to the deeper samples (30-40 m: Table 1). The ore in the upper portion of this profile represents the basal 10m of the current open pit but is considerably richer in Au and W but poorer in Bi, Mo and Se than the corresponding interval sampled in profile P1 (*cf.* Scott and McQueen, 2000). However material from this depth in both profiles are relatively low in Fe, Mn, P, S, As, Cu, Pb, Se and Zn relative to the deeper material, suggesting that abundances of these elements are consistently low in this interval in which kaolinite is strongly developed relative to muscovite (see Scott and McQueen, 2000 and below).

Only the ore interval in RC00CA0602 was analysed but that interval actually passes from totally oxidate material into partially weathered material in which secondary sulfides are developed. The deeper secondary sulfide material contains higher abundances of S, Ag, As, Au, Bi, Co, Cu, Sb, Se and W (*i.e.*, ore associated elements) but lower Al, Mg, Na, K, Ti, Ni and Pb (Table 1).

### 5.2 DD97NC0059

This drill hole was regularly analysed over a 50 m vertical interval, with ore being intersected at the oxidate/supergene sulfide interface at 100 m, *i.e.*, about 30 m deeper than in RC00NC0602. The supergene sulfide zone in this hole is characterised by development of chalcocite and native Cu. Samples from 60-70 m represent barren material outside the peripheral low grade zone at 70-90 m (Figure 3). A prominent Mn-rich interval at about 40 m depth was also sampled, mainly to verify the nature of the Mn minerals (lithiophorite and hollandite: see also McQueen *et al.*, 2001). Table 2 shows that the ore and peripheral low grade zones are enriched in Fe, Mn, P, S, Ag, As, Au, Bi, Cd, Co, (Cu), Ni, Pb, Sb, (Se), W and Zn relative to the barren material. The ore interval, particularly the secondary sulfide zone, is

enriched in Ag, As, Au, Bi, Cd, Co, Cu, Mo, Sb, Se, W and Zn. Lead however attains its maximum in the oxidate portion of the ore interval (Table 2).

**Table 1. Average composition of intervals in drill holes DD97NC0054 and RC00CA0602, New Cobar (ppm, unless otherwise indicated)**

Drill Hole	DD97NC0054			RC00CA0602	
	Ox Ore	Ox Ore	Peripheral	Ox Ore	2° Sulf Ore
True Depth (m)	20-30	30-40	40-50	65-70	70-75
No. of Samples	3	5	6	3	2
Al (%)	0.26	0.83	5.47	5.17	2.65
Fe (%)	4.25	13.7	7.33	6.18	7.58
Mg	120	290	930	890	330
Ca	<50	76	110	73	63
Na	<100	120	200	760	220
K (%)	<0.20	0.24	0.80	0.67	0.46
Ti	660	1500	2700	2200	1200
Mn	110	220	46	99	38
P	60	320	99	<b>210</b>	100
S	130	370	440	2.70%	8.06%
Ag	2.7	3.0	1.0	1.8	9.1
As	52	180	17	84	160
Au (ppb)	6700	5500	10	830	3000
Ba	<100	<100	160	190	<100
Bi	21	120	7	18	79
Cd	0.1	0.2	0.3	0.1	0.1
Ce	12	20	35	71	23
Co	2	3	(3)	27	91
Cr	8	25	62	46	25
Cs	<1	<1	3	3	<1
Cu	420	800	360	3400	1.51%
La	7	9	18	35	12
Mo	1.8	4.2	5.1	2.1	2.9
Ni	<5	<5	32	28	18
Pb	540	1700	1100	<b>940</b>	620
Rb	<20	<20	56	61	22
Sb	4	6	2	2	5
Sc	1	6	9	9	4
Se	9	94	<5	12	30
Sr	2	5	9	14	5
Th	1	4	12	9	5
U	<2	<2	<2	<2	<2
V	5	29	84	54	24
W	61	53	11	49	170
Zn	27	190	<b>66</b>	56	30
Zr	21	48	81	67	36

Note: Values in bold represent averages obtained by omitting one anomalously high value.

**Table 2. Average composition of intervals in drill hole DD97NC0059, New Cobar**  
(ppm, unless otherwise indicated)

<b>Zone</b>	<b>Mn-rich</b>	<b>Barren</b>	<b>Peripheral</b>	<b>Ox Ore</b>	<b>2° Sulf Ore</b>
<b>True Depth (m)</b>	<b>~40</b>	<b>60-70</b>	<b>70-90</b>	<b>90-100</b>	<b>100-110</b>
<b>No. of Samples</b>	<b>1</b>	<b>3</b>	<b>6</b>	<b>5</b>	<b>6</b>
<b>Al (%)</b>	2.50	2.69	4.77	2.69	1.78
<b>Fe (%)</b>	6.66	4.97	10.2	11.3	10.7
<b>Mg</b>	380	1500	<b>190</b>	390	2500
<b>Ca</b>	60	62	93	92	<b>90</b>
<b>Na</b>	110	150	190	300	<100
<b>K (%)</b>	0.33	0.64	0.69	0.28	0.28
<b>Ti</b>	890	970	2200	1400	820
<b>Mn</b>	1.25%	140	470	250	340
<b>P</b>	140	78	150	230	130
<b>S</b>	130	44	170	1400	1.23%
<b>Ag</b>	1.1	0.5	1.2	3.7	<b>3.6</b>
<b>As</b>	5	9	21	<b>47</b>	<b>53</b>
<b>Au (ppb)</b>	14	9	54	2300	2500
<b>Ba</b>	1200	120	170	<100	110
<b>Bi</b>	0.9	0.2	1.9	31	42
<b>Cd</b>	0.2	0.1	0.3	0.7	5.6
<b>Ce</b>	140	26	61	39	21
<b>Co</b>	330	5	9	17	61
<b>Cr</b>	19	31	53	34	21
<b>Cs</b>	2	2	3	1	1
<b>Cu</b>	1700	290	840	2500	<b>3600</b>
<b>La</b>	20	14	24	25	12
<b>Mo</b>	0.7	0.5	0.3	1.3	<b>4.9</b>
<b>Ni</b>	51	12	23	16	17
<b>Pb</b>	<20	<20	450	3200	1400
<b>Rb</b>	39	49	62	26	21
<b>Sb</b>	2	1	2	4	5
<b>Sc</b>	4	5	10	5	4
<b>Se</b>	<5	<5	<5	<b>&lt;5</b>	<b>6</b>
<b>Sr</b>	4	6	11	7	11
<b>Th</b>	3	5	10	6	3
<b>U</b>	<2	<2	3	5	<2
<b>V</b>	34	27	76	62	24
<b>W</b>	13	11	<b>13</b>	48	<b>100</b>
<b>Zn</b>	120	66	110	<b>120</b>	<b>280</b>
<b>Zr</b>	24	30	60	37	23

Note: Values in bold represent averages obtained by omitting one anomalously high value.

### 5.3 DD97NC0060

This hole was drilled on the eastern edge of the peripheral low grade zone and remained in that zone until it intersected the chalcocite-rich top of the supergene sulfide ore at 100 m depth. At 120 m depth, it passed into sphalerite- and chalcopyrite- bearing partially oxidised primary ore before passing out into the peripheral low grade zone again at about 140 m depth (Figure 3). A zone, where disseminated pyrite is still present, occurs at 80-90 m depth.

Despite its strongly elevated S and Cu and anomalous As and Pb, the raft of fresh rock with disseminated pyrite is not Au-mineralised (Table 3). Excluding the chalcocite-rich sample (which is comparatively low in other chalcophile elements, except Cu and perhaps Mo), both the primary and secondary sulfide ore zones contain lower Al, Sc and Th, and higher Fe, S, Ag, As, Au, Cd, Co, Cu, Se and W than the low grade peripheral material (Table 3). Zinc is very abundant in the primary sulfides (Table 3), reflecting the presence of sphalerite. Bismuth is high in both the ore and basal peripheral zones. Molybdenum is also abundant in the peripheral zone within 10 m of ore (Table 3).

Mineralogical features of this profile were determined by X-ray diffraction which indicates that the chlorite, muscovite and siderite of the wall rocks at depth are generally absent from the ore zone. However, even in the primary ore zone assemblages of pyrite ± galena ± sphalerite ± chalcopyrite are sometimes partially weathered to form anglesite and chalcocite at depths below 120 m (Figure 4). Pyrite is the most stable of the sulfides and persists up to within 80 m of the surface but the other primary sulfides do not survive above 120 m depth and secondary Cu minerals, chalcocite and chalcantite ( $\text{CuSO}_4 \cdot 5\text{H}_2\text{O}$ ), and alunite-jarosite minerals are developed in the secondary sulfide zone. Malachite staining occurs in the peripheral low grade zone above 100m (see Appendix 1) and Fe oxides and phyllosilicates are also observed outside the weathered ore zone. Despite the preservation of pyrite in the interval 80-90m, some alunite-jarosites are present and kaolinite, rather than chlorite, is present with the muscovite, *i.e.*, the presence of pyrite does not reflect totally unweathered material.

### 5.4 Electron microprobe studies

Average minor and trace element contents of the Fe oxides in 6 samples are reported in Table 4. This shows that goethite is an important host for Cu and Zn, with Co also being present in the deeper (less weathered) samples. Copper is particularly enriched in the more Al-rich goethites and comparison with the whole rock Cu contents for samples emphasises how good a host such goethite is in samples higher in the profile. In the goethite from deeper than 127 m in DD97NC0059, Cu is present in other phases like native Cu and chalcocite, cuprite. The deeper Al-rich goethites also contain substantial amounts of S close to the site of active weathering of the sulfides but such S within the goethite appears to be lost with further weathering higher in the profile (Table 4). Similarly Pb contents are very much higher in sample 138834 at the site of active weathering than in other samples.

Manganese oxides occur as two mineralogically distinctive types in the New Cobar profile:- Al-rich lithiophorite,  $(\text{Al,Li})\text{MnO}_2(\text{OH})_2$ , and K-Ba-Pb-bearing members of the cryptomelane-hollandite-coronadite solid solution series,  $(\text{K,Ba,Pb})(\text{Mn}^{4+}, \text{Mn}^{2+})_8\text{O}_{16}$ . Lithiophorite is an important host for Cu and Co (Table 5). Whereas members of the cryptomelane-hollandite-coronadite series contain less Cu but substantial Pb, enough in some cases to be classified as coronadite (Table 5, Figure 5). Zinc is retained in these phases, although, in the one case (sample 138769) where data is available from coexisting Mn oxide types, Zn is actually higher in the lithiophorite (Table 5), as generally found in previous studies.

**Table 3. Average compositions of intervals in drill hole DD97NC0060, New Cobar**  
(ppm, unless otherwise indicated)

Zone	Diss Py	Peripheral	Chalcocite	Sulf Ore	Sulf Ore	Peripheral
True Depth (m)	80-90	90-98	100	100-120	120-140	>140
No. of Samples	3	5	1	8	13	2
Al (%)	9.72	5.76	4.45	2.38	2.77	3.95
Fe (%)	2.46	3.95	6.64	9.80	8.88	8.28
Mg	5800	580	120	<b>1000</b>	6500	1.75%
Ca	65	100	220	70	99	95
Na	400	260	110	<100	110	100
K (%)	3.08	0.40	<0.20	<0.20	0.38	0.32
Ti	4200	1900	1100	840	1400	1900
Mn	120	1700	13	170	580	1200
P	130	200	70	60	83	84
S	1.25%	640	9.17%	5.13%	5.02%	6300
Ag	0.3	1.9	2.0	<b>3.2</b>	11	1.3
As	42	63	290	200	110	<1
Au (ppb)	11	<b>170</b>	280	<b>1300</b>	2900	150
Ba	470	140	<100	<100	110	100
Bi	7	9	28	<b>24</b>	58	70
Cd	0.2	0.7	0.4	2.2	8.4	0.3
Ce	85	<b>35</b>	26	23	32	45
Co	20	<b>26</b>	75	94	72	21
Cr	88	44	20	21	34	43
Cs	9	1	<1	<1	2	1
Cu	2200	1500	26.9%	4100	1.10%	170
La	48	18	11	12	15	22
Mo	0.8	3.0	6.1	3.4	1.9	15
Ni	38	11	30	14	24	18
Pb	310	2100	380	<b>260</b>	<b>160</b>	180
Rb	230	28	<20	<20	36	26
Sb	2	3	7	3	6	5
Sc	16	8	5	5	5	7
Se	<5	<b>&lt;5</b>	94	24	19	5
Sr	17	13	5	7	9	18
Th	17	10	6	4	6	8
U	2	5	<2	<2	<2	<2
V	100	56	48	38	36	53
W	9	40	14	<b>33</b>	110	13
Zn	73	140	170	190	<b>1700*</b>	390
Zr	120	51	31	23	42	60

Note: Values in bold represent averages obtained by omitting one anomalously high value,  
\* indicates two high values omitted.

**Table 4. Average minor and trace element contents in goethite and hematite, New Cobar (ppm, unless otherwise indicated) – determined by electron microprobe.**

Sample	Drill hole/ depth (m)	Fe Oxide	No. of Analyses	Co	Cu	Pb	Ni	Zn	SO <sub>3</sub> %	Al <sub>2</sub> O <sub>3</sub> %	Cu content whole rock (ppm)	Cu content Goethite/Cu content rock
138521	P2:4.9	Goethite	3	<140	7700	3700	<140	4400	0.08	0.32	8600	0.9
		Al-Goethite	7	<140	1.93%	4900	<140	2000	0.17	1.85		2.2
138416	10m	Al-Goethite	6	<140	1.67%	5200	<140	1600	0.14	2.94	1800	9.3
NC14	~30m?	Goethite	2	210	4800	2100	200	7000	0.10	0.60	-	-
		Goethite	3	<140	1.17%	<1000	140	670	0.15	0.97		-
138749	NC0059:56	Al-Goethite	8	<140	5900	<1000	<140	220	0.18	2.01	1700	3.5
		Al-Goethite	1	<140	2.12%	1300	160	1400	0.22	3.49		12
138834	NC0059:127	Goethite	5	280	4900	1.86%	<140	5500	0.07	1.36	6.54%	<0.1
		Al-Goethite	4	180	2.27%	1.27%	160	5700	1.02	3.06		0.3
138768	NC0059:130	Goethite	6	<140	<160	1100	<140	910	0.09	<0.04	1600	<0.1
		Al-Goethite	4	290	1800	3400	<140	2200	2.39	3.43		1.1
138749	NC0059:56	Hemetite	1	<140	3700	<1000	<140	<190	0.17	1.42	1700	2.2
138768	NC0059:130	Hematite	3	160	<160	1900	<140	220	0.04	0.31	1600	<0.1

**Table 5. Average compositions of Mn oxide phases, New Cobar (wt%)  
– determined by electron microprobe**

Sample True Depth (m) Phase No. of Analyses	138416 10 Pb-K 3	138521 4.9 K-Ba      Pb 6              2		NC14 ~30m ? Lithiophorite 3	138769 110 Ba      Lithiophorite 5              5	
SiO <sub>2</sub>	0.51	0.18	0.16	0.11	0.37	0.11
Al <sub>2</sub> O <sub>3</sub>	1.79	1.27	0.85	24.0	5.76	22.0
Fe <sub>2</sub> O <sub>3</sub>	3.13	<0.02	<0.02	0.89	<0.02	0.46
MnO <sub>2</sub>	87.0	91.5	82.1	73.6	92.9	70.5
CoO	0.39	0.47	0.22	0.16	0.29	4.31
MiO	<0.02	<0.02	<0.02	<0.02	<0.02	0.08
CuO	2.26	2.77	3.00	7.44	2.24	3.69
ZnO	0.20	0.34	0.22	0.07	0.07	0.16
PbO	9.75	10.0	19.0	<0.10	0.61	<0.10
CaO	0.14	0.04	0.02	<0.01	0.03	0.01
BaO	0.82	2.70	0.56	0.04	8.69	0.26
K <sub>2</sub> O	3.22	1.80	0.29	<0.01	1.68	0.04

Sample 138834 (DD97NC0059:127 m) contains chalcocite-djurleite with a composition of Cu<sub>1.84</sub>Fe<sub>0.02</sub>S<sub>1.00</sub>, veined, rimmed and replaced by goethite. It also contains native Cu which is commonly rimmed by cuprite, Cu<sub>2</sub>O.

Sphalerite from the partially weathered sample 138731 (DD97NC0060:147 m) contains 10 atomic percent Fe.

## 6. Discussion

### 6.1 Weathering of the New Cobar ore

Primary sulfide-rich mineralisation consists of assemblages of Au + pyrite + pyrrhotite + chalcopyrite + sphalerite + galena + Bi sulfides + magnetite (P.A. Leah, pers. comm., 1999). However, at depths above about 120 m, all the primary sulfides (except pyrite) appear to be susceptible to acidic weathering, although perched sulfides may occur up to 70m in RC00CA0602 (Table 1, Figure 6), possibly due to armouring by silicification, although textural confirmation was not possible for these samples. The primary sulfides weathered to form secondary sulfides (*e.g.* chalcocite), sulfates (*e.g.* anglesite and chalcantite) and complex alunite-jarosite minerals (*e.g.* hinsdalite) and Mn oxides or have been totally destroyed and constituent elements dispersed (*e.g.* loss of Zn when sphalerite breaks down). However, even when secondary Cu and Pb minerals are not obvious in weathered high grade ore samples, gossanous textures are present above the base of complete oxidation (Figure 6). Casts after pyrite are also obvious in the lower grade peripheral material to similar depths. Malachite appears to form in the peripheral parts of the deposit (Figure 6) where oxidation of disseminated pyrite would have generated a less acidic environment than in the lode ore.

The bulk of the original gold was associated with Bi minerals and contained some Ag (Section 1) but the Ag contents and Au/Ag ratios in the weathered lode from 20-40 m is relatively depleted in Ag (Table 6). However, above 15 m, Scott and McQueen (2000) found that Au is severely depleted and Ag substantially retained *i.e.*, Au and Ag behave quite differently at different levels in the weathering profile. Thus, Ag is depleted relative to Au above 40m (and possibly above 65 m) and then Au itself depleted above 15 m. The current arid conditions and resultant Cl-rich groundwaters of the region would facilitate separation of Ag from Au during weathering (*e.g.*

Mann, 1984; Webster and Mann, 1984). Thus, this study allows the behaviour of Au and Ag to be documented through the whole profile, although sampling of the ore between 40 and 65 m is needed to more accurately define at what level Ag is freed from its association with Au. Confirmation that Au is actually lost (in an absolute sense) close to the surface during weathering might be afforded by detailed mass balance calculations (see Gray and Sergeev, 2001).

**Table 6. Average composition of ore at various depths in the profile at New Cobar**  
(from Tables 1-3 and Scott and McQueen, 2000: ppm, unless otherwise indicated)

	Profile P1		DD97NC0054		RC00CA0602		DD97NC0059		DD97NC0060	
Ore Type	Oxide	Oxide	Oxide	Oxide	Oxide	2° Sulf Ore	Oxide	2° Sulf Ore	2° Sulf Ore	1° Sulf Ore
Depth (m)	0-15	15-20	20-30	30-40	65-70	70-75	90-100	100-110	100-120	120-140
Al (%)	1.48	0.96	0.26	0.83	5.17	2.65	2.69	1.78	2.38	2.77
Fe (%)	12.8	15.6	4.25	13.7	6.18	7.58	11.3	10.7	9.80	8.88
Mg	590	310	120	290	890	330	390	2500	<b>1000</b>	6500
Ca	61	<50	<50	76	73	63	92	<b>90</b>	70	99
Na	260	150	<100	120	760	220	300	<100	<100	110
K (%)	0.37	0.20	<0.20	0.24	0.67	0.46	0.28	0.28	<0.20	0.38
Ti	1300	730	660	1500	2200	1200	1400	820	840	1400
Mn	60	69	110	220	99	38	250	340	170	580
P	110	88	60	320	<b>210</b>	100	230	130	60	83
S	490	630	130	370	2.70%	8.06%	1400	1.23%	5.13%	5.02%
Ag	1.0	1.5	2.7	3.0	1.8	9.1	3.7	<b>3.6</b>	<b>3.2</b>	11
As	130	44	52	180	84	160	<b>47</b>	<b>53</b>	200	110
Au (ppb)	110	2360	6700	5500	830	3000	2300	2500	<b>1300</b>	2900
Ba	<100	<100	<100	<100	190	<100	<100	110	<100	110
Bi	57	38	21	120	18	79	31	42	<b>24</b>	58
Cd	0.5	0.3	0.1	0.2	0.1	0.1	0.7	5.6	2.2	8.4
Ce	26	20	12	20	71	23	39	21	23	32
Co	3	3	2	3	27	91	17	61	94	72
Cr	37	29	8	25	46	25	34	21	21	34
Cs	1	<1	<1	<1	3	<1	1	1	<1	2
Cu	<b>680</b>	1300	420	800	3400	1.51%	2500	<b>3600</b>	4100	1.10%
La	13	7	7	9	35	12	25	12	12	15
Mo	11	27	1.8	4.2	2.1	2.9	1.3	<b>4.9</b>	3.4	1.9
Ni	<10	<10	<5	<5	28	18	16	17	14	24
Pb	730	990	540	1700	<b>940</b>	620	3200	1400	<b>260</b>	<b>160</b>
Rb	29	22	<20	<20	61	22	26	21	<20	36
Sb	7	5	4	6	2	5	4	5	3	6
Sc	8	9	1	6	9	4	5	4	5	5
Se	23	81	9	94	12	30	<b>&lt;5</b>	<b>6</b>	24	19
Sr	7	5	2	5	14	5	7	11	7	9
Th	6	3	1	4	9	5	6	3	4	6
U	<2	2	<2	<2	<2	<2	5	<2	<2	<2
V	32	19	5	29	54	24	62	24	38	36
W	11	52	61	53	49	170	48	<b>100</b>	<b>33</b>	110
Zn	62	49	27	190	56	30	<b>120</b>	<b>280</b>	190	<b>1700</b>
Zr	48	26	21	48	67	36	37	23	23	42
Au/Ag	0.1	1.6	2.5	1.8	0.5	0.3	0.6	0.3	0.6	0.3

Note: Values in bold represent averages obtained by omitting one or two anomalously high value(s).



The primary and secondary sulfide ores generally have higher Mg, S, Ag, Cd, Co, Cu, W and Zn than the oxidised ore, although Mg, Cd and Zn are depleted in the perched secondary sulfides in RC00CA0602 (Table 6). Of these elements, Zn and Cd are strongly mobilised as soon as the primary sulfides weather, whereas Cu is more progressively lost and Mo and W appear to be retained with the supergene sulfides at 100-110 m. However, variations in the other elements are less regular and may reflect original mineralogical variations in the ore. Selenium appears to be concentrated above 40 m depth *i.e.*, implying separation from S with which it is usually associated. Aluminium, Co, Cu, La and Ni contents are also very much lower above 40 m (Table 6). Manganese shows some tendency to be more abundant in the ore below 90 m (see also below).

## 6.2 Mineralogical variations in the regolith profile

Scott and McQueen (2000) indicated that kaolinite was relatively depleted above 20 m in the P1 and P2 profiles. This study indicates that Al is depleted above 40 m (and perhaps above 65 m) and could imply that Al-depletion could be related to strong (*i.e.*, complete) weathering of the sulfides at New Cobar. However, examination of the nature of the Al-bearing minerals above the base of complete weathering indicates a complex distribution of kaolinite and muscovite (Figure 8) with kaolinite being the dominant Al-bearing phase, except in the top 20 m in P1 and P2 and DD97NC0059 (*i.e.*, on the edges of the alteration zone about the New Cobar Lode.) Significant amounts of Al are also incorporated into Fe oxides (Scott and McQueen, 2000; Table 4). However, if strong kaolinite development is associated with the weathered ore and more muscovitic assemblages occur more peripherally in the top 20 m of the regolith, this feature could potentially be used during exploration, perhaps by use of a PIMA (Portable Infrared Mineral Analyser).

The extent of silicification and quartz veins was also mapped out (Figure 8) but samples probably do not extend far enough away from the mineralisation to observe any variation in Si abundance with proximity to ore. As indicated above, the effect of silicification in helping to preserve perched sulfides needs to be tested by additional sampling of drill core in the 40-65 m depth interval. Additional information on the relationship between siliceous samples and mineralisation can probably be obtained from paramagnetic studies of the quartz-rich and silicified samples (see van Moort *et al.*, 1996).

Manganese is quite abundant in the primary ore and fresh peripheral material in DD97NC0060 (Table 3) and in the partially weathered zone in DD97NC0059 (Table 2). In the fresh material, Mn might be expected to occur in chlorite (Stegman and Pocock, 1996) and perhaps, siderite (see also Figure 4) and to be freed during weathering and stabilised as K-Ba-Pb-bearing members of the cryptomelane-hollandite-coronadite solid solution series and Al-rich lithiophorite along fractures in the deposit (McQueen *et al.*, 2001). Figure 9 shows that Mn >500ppm is present intermittently at various levels in the regolith profile with some tendency for development of the Mn oxides on the periphery of the high grade ore zone. Figure 5 appears to show that the deeper Mn oxide is not as Pb-rich as the cryptomelane-hollandite-coronadite members higher in the profile. This could suggest that the Mn oxides higher in the profile formed when more Pb was available, possibly incorporating Pb freed when earlier weathering products were destroyed/modified. Because of the Pb halo about the deposit and its implications for both exploration and environmental concerns, the abundance of Pb-rich Mn oxides should be better documented. Furthermore, because lithiophorite, in particular, is a good host for Cu which can affect the efficiency of cyanide during processing, more work on documenting the various Mn oxides in the New Cobar profile should be considered.

The high contents of Cu, Pb, Zn and S in the goethite that has replaced sulfides in the top of the supergene sulfide zone (Table 4) suggests that these components were transferred directly to the goethite during oxidation. However their lower abundances higher in the profile suggest that further weathering leaches some of these impurities.

A summary of how various elements are redistributed into neo-formed minerals during weathering of the New Cobar deposit is presented in Figure 10.

### 6.3 Features in the peripheral zone

Disseminated pyrite occurs peripherally to the ore lode, as indicated in Figure 5, when oxidised, this can be readily identified as Fe-rich cubic casts for up to 80 m from the high grade ore. The fresh pyrite contains significant amounts of As, Bi and Cu (Table 3) and, although its Au content is low, it is probably related to the late stage pyrite event which occurred after the main Au-mineralising event (Leah and Roberts, 2000).

Comparison of data from the P1 and P2 profiles indicate significant Pb contents for at least 25 m from the lode with such anomalism likely to be present in surface samples (Scott and McQueen, 2000). However surface disturbance in the vicinity of the New Cobar deposit precludes using the current surface samples to better determine the lateral extent of the anomalism. Thus shallow depth samples from DD97NC0059 and DD97NC0060 plus RC00CA0602 were analysed and used with company data from several drill holes within 500 m about the deposit. Results (Figure 11) suggest that the Pb anomaly about the lode is present for up to 70 m south of the 1999 pit but is not so well developed east of the lode. The absence of data from immediately west of the pit does, however, still leave the width of the Pb anomaly poorly constrained, especially as the southern anomalous Pb contents could represent a weakly mineralised southern extension of the economic mineralisation.

## 7. Conclusions and Recommendations

Weathering at the New Cobar Cu-Au deposit appears to reflect two major events – an initial period of acidic weathering and subsequent Cl-overprinting under arid conditions. The initial weathering occurred under acidic conditions generated by the oxidation of the pyrite-rich sulfide assemblages and resulted in the formation of secondary sulfides, sulfates and alunite-jarosite minerals below the base of complete oxidation and sulfate- and base metal-rich Fe oxides above the base of complete oxidation. During this process of formation of a mature gossan profile elements like Co, Cu, Ni and Zn have been progressively lost up the profile. The later Cl-rich weathering event occurred under more arid conditions and resulted in Cl-bearing minerals like pyromorphite being formed at the expense of pre-existing secondary phases. Under the influence of Cl-rich groundwaters, Ag was separated from, and depleted relative to, Au above 40 m (and possibly above 65 m) and then Au itself was lost above 15 m. This two-stage weathering history, with Au being severely affected by the second stage in near surface material, and potential pathfinder elements, like Cu, being affected mostly by the earlier weathering processes, has implications for the interpretation of regional geochemical surveys.

Fortunately for geochemical exploration, the abundances of Ag, As, Bi, Cu, Mo, Pb, Sb, Se and W are still elevated in the surficial samples at New Cobar (Scott and McQueen, 2000). These elements persist to the surface in readily detectable amounts and can give confidence in

interpreting relatively low Au contents as significant during an exploration programme in the Cobar region. Although some elements appear to be progressively lost with increased weathering up the profile, others like Zn, Cd and are substantially lost at the site of active weathering with the breakdown of the sulfides. Other elements like Mo and W are concentrated at 100-110 m in the secondary sulfides zone whereas Se is concentrated above 40 m *i.e.*, it is separated from S which it normally follows.

Scott and McQueen (2000) also indicated that Pb >700 ppm occurs up to 25 m from the ore and suggested that the presence of an extensive Pb halo might be useful for regional exploration. This study of the distribution of near-surface Pb contents indicates that abundances >300ppm extend up to 70 m south of the mineralisation.

Strong development of kaolinite surrounded by more muscovitic assemblages in surficial samples may also be a feature of a weathered ore zone in this region

Because this study did not thoroughly sample the ore in the interval 40-65m, definition of exactly where in the profile Ag commences to be depleted relative to Au is not known. Similarly, questions about Al, Co, Cu, La and Ni depletion and possible Se enrichment and silicification in this interval need to be addressed by additional sampling.

## **8. Acknowledgements**

Peak Gold Mines geologists (especially Peter Leah) are thanked for facilitating the collection of samples and providing background information for this study. Partial funding for this study was provided by Peak Gold Mines Pty Ltd.

Samples were crushed by Jeff Davis and X-ray diffraction traces were prepared by Tin Tin Win. Figures were drawn by Chris Taylor and the text and tables formatted by Sue Crammond (all at CSIRO, Exploration and Mining, North Ryde).

Polished section were prepared by Glen Fisher (UC) and analysed on the electron microprobe of the Research School of Earth Sciences at ANU, Canberra, taking advantage of the facility maintained by Nick Ware.

An earlier draft of the text was reviewed by Peter Leah, Craig Roberts and Colin Pain.

## 9. References

- Glen, R.A., 1991. Inverted transtensional basin setting for Gold and Base metal deposits at Cobar, New South Wales. *BMR Journal of Geology and Geophysics*, 120: 13-24.
- Gray, D.J. and Sergeev, N.B., 2001. Gold mass balance in the regolith, Mystery Zone, Mt. Percy, Kalgoorlie, Western Australia. *Geochemistry: Exploration, Environment, Analysis*, 1 (in press)
- Leah, P.A., 1996. Relict Lateritic Weathering Profiles in the Cobar District, NSW. *In The Cobar Mineral Field - A 1996 Perspective* (Eds: W.G. Cook *et al.*), Australasian Institute of Mining and Metallurgy, Melbourne. pp.157-177.
- Leah, P.A. and Roberts, C.A., 2000. New Cobar pit. *In Central West Symposium Cobar 2000, Cobar field trip guide* (Ed: M.J. Spry) CRC LEME, Perth. pp.8-12.
- McQueen, K.G., Scott, K.M., Ogilvie, P.G. and Crowther, B.R., 2001. Atlas of regolith materials from the weathered zone, New Cobar Deposit. CRC LEME Restricted Report 162R/CSIRO Exploration and Mining Report 815R (25pp).
- Mann, A.W., 1984. Mobility of gold and silver in lateritic weathering profiles: some observations from Western Australia. *Economic Geology*, 79: 38-49.
- Scott, K.M. and McQueen, K.G., 2000. The mineralogy and geochemistry of New Cobar Au-Cu mineralisation in the regolith and exploration implications for the Cobar district, western NSW. CRC LEME Restricted Report 137R/CSIRO Exploration and Mining Report 728R (25pp).
- Stegman, C.L., 2000. The New Occidental deposit: variation on a theme. *In Central West Symposium Cobar 2000, Extended Abstracts* (Eds: K.G. McQueen and C.L. Stegman) CRC LEME, Perth. pp. 107-112.
- Stegman, C.L. and Pocock, J.A., 1996. The Cobar Goldfield – A Geological Perspective. *In The Cobar Mineral Field - A 1996 Perspective* (Eds: W.G. Cook *et al.*), Australasian Institute of Mining and Metallurgy, Melbourne. pp.229-264.
- Stegman, C.L. and Stegman, T.M., 1996. The History of Mining in the Cobar Field. *In The Cobar Mineral Field - A 1996 Perspective* (Eds: W.G. Cook *et al.*), Australasian Institute of Mining and Metallurgy, Melbourne. pp.3-39.
- Webster, J.G. and Mann, A.W., 1984. The influence of climate, geomorphology and primary geology on the supergene migration of gold and silver. *Journal of Geochemical Exploration*, 22: 21-42.
- Van Moort, J.C., Li, X., Pwa, A., Bailey, G.M., Russell, D.W. and Butt, C.R.M., 1999. The use of electron paramagnetic resonance spectra and geochemical analysis of acid insoluble residues for recognising primary alteration haloes of gold mineralisation in the regolith. *In New Approaches to an Old Continent. Proceedings of Regolith '98.* (Eds. G. Taylor and C. Pain), CRC LEME, Perth. pp. 67-76.

## Appendix 1

### Sample descriptions, New Cobar - DD97NC054

Sample No.	Depth (m)	Description
138661	0.5-0.6	Fawn brown siltstone
138662	1.5-1.6	Yellow-brown siltstone with red staining adjacent to fracture
138663	5.0-5.1	Buff and yellow-red siltstone, some fine qtz veinlets with casts after py. Smectite along fractures
138664	7.0-7.1	Red ferruginous siltstone cut by qtz veinlets.
138665	10.3-10.4	Pale purple siltstone cut by qtz veinlets. Black staining + blue coating along fracture
138666	14.4-14.5	Qtz vein with red Fe staining cutting purple siltstone. Cast after py
138667	18.2-18.3	Purple siltstone cut by qtz veins, late stage qtz vein has casts after py
138668	23.8-23.9	Pale grey siliceous siltstone cut by red Fe staining containing py casts
138669	28.5-28.6	Grey and purple siltstone cut by red staining
138670	29.6-29.7	Red ferruginous siltstone cut by gossanous vein
138671	34.2-34.3	Buff siliceous siltstone cut by gossanous vein
138672	36.2-36.3	Buff siliceous siltstone cut by gossanous vein
138673	40.5-40.6	Brecciated buff siliceous siltstone cut by gossanous veins
138674	43.0-43.1	Pale purple siliceous siltstone cut by gossanous qtz veins
138675	46.5-46.6	Gassanous qtz vein
138676	48.0-48.1	Pink siliceous siltstone cut by qtz veins with py casts
138677	49.9-50.0	Red-brown brecciated silicified gossan
138678	52.0-52.1	Red-brown brecciated silicified gossan in yellow-brown siltstone
138679	53.8-53.9	Buff brown siltstone cut by qtz veins with py casts
138680	56.0-56.1	Purple siliceous siltstone cut by qtz veins with py casts
138681	57.1-57.8	White and purple siltstone cut by qtz veins with py casts
138682	60.0-60.1	Pink purple siliceous siltstone cut by red Fe diffusion bands
138683	62.1-62.2	Pink siliceous siltstone cut by qt and Fe veins (both with py casts)
138684	64.0-64.1	Purplish siliceous siltstone cut by qtz veins (with py casts) and Fe diffusion bands
138685	65.8-65.9	Purplish siliceous siltstone cut by Fe diffusion bands. White staining along fractures
138686	68.0-68.1	Pink grey siltstone with casts often py, Fe diffusion about veins
138687	72.9-73.0	Grey siltstone
138688	74.0-74.1	Grey and purple siltstone with disseminated py casts
138689	77.0-77.1	Grey and purple siltstone

**Sample descriptions, New Cobar - DD97NC060**

<b>Sample No.</b>	<b>Depth (m)</b>	<b>Description</b>
138690	0.8-0.9	Red siltstone cut by thick qtz veins
138691	5.1-5.2	Red siltstone cut by thick qtz veins
138692	11.3-11.4	Red siltstone cut by qtz veins with py casts. White staining along fracture
138693	15.4-15.5	Purple siltstone cut by qtz veins with py casts. Black Mn staining
138694	21.0-21.1	Red and yellow-brown siltstone cut by qtz veins with py casts
138695	30.2-30.3	Red and yellow-brown siltstone cut by qtz veins with py casts. Yellow diffusion is about a veinlet and appears later
138696	39.7-39.8	Pink-purple siltstone with yellow-red diffusion about veinlet
138697	42.4-42.5	Red siltstone with qtz veins (py casts). Black Mn diffusion about fracture and vein
138698	47.8-47.9	Red siltstone cut by qtz veins (py casts) and later thick qtz veins
138699	55.8-55.9	Red-purple siltstone cut by qtz vein with py casts. White along fractures
138700	65.0-65.1	Pink-red siltstone cut by qtz veins with py casts
138701	71.1-71.2	Pink siltstone cut by qtz veins with py casts and yellow goethitic diffusions out from veins/fractures
138702	74.0-74.1	Pink-grey siltstone cut by qtz veins (py casts) and rimmed by Fe staining. White along fractures
138703	81.9-82.0	Grey siltstone cut by qtz-py veinlets. Disseminated py?
138704	84.0-84.1	Grey siltstone with disseminated py. Cut by yellow-red diffusion about veinlet
138705	86.0-86.1	Grey siltstone with disseminated py
138706	88.0-88.1	Grey-purple siltstone with disseminated py
138707	90.5-95.6	Grey-purple siltstone cut by qtz veins. Disseminated py?
138708	93.0-93.1	Grey-purple siltstone with py casts. Pale green Cu staining
138709	94.0-94.1	Purple siltstone cut by qtz/Fe veinlets. Casts after disseminated py. Green Cu staining
138710	99.0-99.1	Pale grey-purple siltstone with disseminated py casts and gossanous veinlets
138711	102.0-102.1	Grey-purple siltstone cut by qtz veins
138712	104.5-104.6	Pale grey siltstone cut by qtz veins with sulfide casts. Green Cu staining
138713	105.0-105.1	Pale grey siltstone. Green Cu staining
138714	108.0-108.1	Purple siltstone cut by qtz/Fe vein breccia. Casts after sulfide
138715	110.2-110.3	White siliceous siltstone cut by qtz/chalcocite vein and rimmed by red Fe oxide
138716	112.0-112.1	Pale grey siltstone cut by qtz/py veins and red Fe diffusion about veins
138717	114.0-114.1	White siltstone cut by qtz/py veins, rimmed by Fe diffusion
138718	115.0-115.1	Pale pink-grey siltstone cut by gossanous qtz veins (with residual py)
138719	117.5-117.6	Grey siliceous siltstone cut by qtz/py/Fe oxide veins. Fe diffusion about veins
138720	120.0-120.1	Green-grey siltstone cut by qtz/py veins
138721	123.2-123.3	Qtz/py vein with green Cu staining (chalcantinite)
138722	125.2-125.3	Qtz vein with py and green-grey siltstone
138723	128.0-128.1	Qtz/py vein
138724	130.1-131.2	Qtz/py vein in grey siltstone
138725	132.2-132.3	Qtz/py vein in grey siltstone
138726	134.2-134.3	Qtz vein/breccia with some pyrite in grey siltstone
138831	138.0-138.1	Py +chalcocite in vuggy qtz vein
138727	140.0-140.1	Porous qtz vein/breccia with some py and chalcocite and grey siltstone fragments
138728	142.2-142.3	Grey siltstone with disseminated py cut by qtz/py veins
138729	144.1-144.2	Grey siltstone cut by qtz/py veinlets and qtz/py vein
138730	146.0-146.1	Grey siltstone cut by qtz/py vein, disseminated py in rock
138731	147.5-147.6	Grey leached siltstone cut by barren qtz vein
138732	148.0-148.1	Grey leached siltstone. White along fractures
138733	150.1-150.2	Grey siliceous siltstone with disseminated sulfides cut by qtz/py veins
138832	151.8-151.9	Chalcopyrite/sphalerite in white qtz vein
138734	153.8-153.9	Grey siliceous siltstone cut by qtz/py veins
138735	156.5-156.6	Grey siliceous siltstone (with disseminated sulfides) cut by qtz/py veins
138736	158.0-158.1	Qtz vein/breccia with py and grey siltstone

**Sample descriptions, New Cobar - DD97NC059**

<b>Sample No.</b>	<b>Depth (m)</b>	<b>Description</b>
138737	0-0.1	Red-brown siltstone with disseminated py casts
138738	4.0-4.1	Grey-purple siliceous siltstone with disseminated py casts
138739	5.0-5.1	Red-purple siltstone with disseminated py casts
138740	10.0-10.1	Red siltstone cut by qtz veinlets (with py casts). Yellow-red diffusion
138741	15.0-15.1	Red siltstone cut by qtz veins. Black staining along fractures
138742	20.7-20.8	Brown siltstone cut by qtz veins. Red Fe diffusion
138743	26.0-26.1	Brown siltstone cut by qtz veinlets, red Fe diffusion. Black Mn staining
138744	31.0-31.1	Brown siltstone cut by qtz veinlets with py casts. Red diffusion about veins
138745	35.6-35.7	Brown siltstone cut by gossanous Fe bands
138746	38.2-38.3	Pink siltstone with qtz veinlets (+ py casts), disseminated py casts. Red Fe diffusion and white coating on fractures
138833	48.5-48.6	Py and magnetite with qtz veinlets in carbonaceous shale
138747	49.0-49.1	Red siltstone cut by qtz veins (+ py casts). Black Mn coated by kaolinite on fractures
138748	50.0-50.1	Red siltstone cut by qtz veins. Coated by Mn + kaolinite
138749	56.0-56.1	Red siltstone cut by qtz veins. Black Mn oxide + kaolinite coating
138750	59.5-59.6	Pale purple siltstone with disseminated py casts cut by qtz/Fe oxide vein. Red Fe diffusion. Kaolinite along fractures
138751	70.3-70.4	Red siltstone cut by qtz veins. Kaolinite along fractures
138752	81.4-81.5	Qtz/Fe breccia (gossanous)
138753	82.2-82.3	Qtz vein with red Fe patches
138754	84.8-84.5	Red siltstone cut by qtz veins (+sulfide casts). Mn diffusion
138755	88.2-88.3	Pale purple leached siltstone cut by qtz/Fe veins. Fe diffusion about veins
138756	90.7-90.8	Pale purple siltstone cut by qtz/Fe veins. Fe diffusion about veins
138757	95.2-95.3	Pink siltstone with disseminated py/fine veinlet casts. Yellow-red diffusion
138758	98.1-98.2	Red siltstone brecciated by barren qtz veins
138759	102.0-102.1	Pale purple siltstone cut by qtz veins with py casts
138760	104.7-104.8	Purple siliceous siltstone cut by qtz (+ py casts) veins
138761	107.0-107.1	Pale purple siltstone cut by qtz (gossanous) veins. Fe diffusion about veins
138762	110.4-110.5	Pale purple siltstone cut by gossanous qtz veins. Green fibrous malachite
138763	112.2-112.3	Brecciated qtz vein with gossanous patches
138764	113.2-113.3	Purple silicified siltstone cut by gossanous qtz veins. Malachite along fractures
138765	117.5-117.6	Pale pink leached siltstone cut by gossanous qtz veins with green malachite needles. Trace residual py
138766	121.0-121.1	Grey siltstone cut by barren qtz vein. Disseminated py
138767	123.6-123.7	Grey siltstone with disseminated py in barren qtz vein
138834	127.0-127.1	Chalcocite and native Cu in red siltstone cut by qtz veins
138768	130.1-130.2	Gossanous qtz vein with some residual pyrite
138769	134.1-134.2	Pink grey shale cut by qtz/weathering sulfide vein

**Appendix 2 Composition of samples, DD97NC0054 and RC00CA0602, New Cobar (ppm, unless indicated otherwise)**

NC0054	Depth(m)	Al%	Fe%	Mg	Ca	Na%	K%	Ti	Mn	P	S	Ag	As	Au ppb	Ba	Bi	Br
138670	30	3.05	16.80	465	<50	0.015	0.51	2200	130	370	560	<0.1	61.20	28.9	<100	3.2	<1
138671	34	0.29	3.44	105	<50	<0.01	<0.2	565	78	74	96	1.2	22.00	2360.0	<100	11.9	<1
138672	36	0.25	3.29	165	60	<0.01	<0.2	570	115	76	135	2.1	56.30	2720.0	<100	40.1	<1
138673	41	0.24	6.01	94	60	0.011	<0.2	835	120	44	150	4.7	77.60	15000.0	<100	10.8	<1
138674	43	0.79	10.10	380	65	0.012	0.37	2220	525	265	305	0.5	164.00	64.5	<100	18	<1
138675	47	0.24	17.40	80	70	0.010	<0.2	540	64	56	420	5.3	193.00	25100.0	<100	97.4	<1
138676	48	1.52	2.87	755	70	0.016	0.55	2960	105	235	86	0.4	26.60	42.0	200.0	4.5	<1
138677	50	0.81	15.50	145	95	0.016	<0.2	1170	335	500	245	7.5	306.00	671.0	<100	42.3	1.19
138678	52	0.79	22.80	58	80	<0.01	<0.2	635	41	515	785	1.5	194.00	1550.0	<100	421	1.06
138679	54	3.1	7.95	720	85	0.027	0.68	1530	60	56	390	1.4	3.89	10.7	158.0	15.7	<1
138680	56	8.7	11.00	1390	155	0.027	1.20	3950	35	98	580	2	17.00	18.2	155.0	2.8	<1
138681	57	6.65	6.00	125	80	<0.01	<0.2	2730	26	80	315	0.9	55.50	12.3	<100	14.2	1.16
138682	60	5.15	4.70	1230	115	0.025	1.15	2800	42	125	305	0.4	6.91	6.1	280.0	3.7	1.62
138683	62	4.8	9.08	845	75	0.016	0.69	2420	71	68	265	0.2	13.60	<5	120.0	2.7	<1
138684	64	4.5	5.23	1250	120	0.022	0.97	2490	39	155	765	1.2	4.29	9.6	207.0	3	<1

NC0054	Depth(m)	Cd	Ce	Co	Cr	Cs	Cu	Eu	Hf	Ir	La	Lu	Mo	Ni	Pb
138670	30	0.1	17.50	<1	137.0	1.93	65	<0.5	2.46	<20	7.87	0.20	0.6	19	1980
138671	34	0.2	10.00	1.02	5.4	<1	631	<0.5	0.65	<20	6.04	<0.2	1.6	<5	510
138672	36	<0.1	12.10	1.22	6.9	<1	201	<0.5	0.81	<20	6.65	<0.2	2.2	<5	600
138673	41	0.2	14.40	3.17	13.3	<1	421	<0.5	1.91	<20	6.98	<0.2	1.5	<5	500
138674	43	0.1	34.70	1.65	24.9	1.76	182	0.67	4.28	<20	18.40	0.21	1.3	9	1600
138675	47	0.3	9.90	3.80	24.4	<1	559	0.62	1.27	<20	4.53	<0.2	5.1	<5	2460
138676	48	0.1	17.80	1.20	19.6	2.10	70	0.72	3.94	<20	11.20	0.25	1.9	<5	855
138677	50	0.2	22.50	2.90	17.0	<1	1400	<0.5	1.69	<20	7.64	<0.2	3.1	<5	1790
138678	52	0.2	11.50	1.32	37.0	<1	1770	0.60	1.02	<20	4.21	<0.2	9.4	<5	1620
138679	54	0.7	33.50	71.30	42.4	2.59	1335	0.95	1.61	<20	6.67	0.22	2.5	55	1350
138680	56	0.3	55.40	2.19	96.4	3.93	189	1.03	5.61	<20	31.10	0.36	3.1	33	1820
138681	57	0.2	23.50	6.49	73.8	<1	195	<0.5	3.55	<20	18.10	<0.2	23.1	51	1080
138682	60	0.2	28.50	2.38	54.5	4.07	90	<0.5	4.34	<20	17.00	0.23	0.6	18	790
138683	62	0.2	31.60	1.72	51.7	2.37	53	0.57	2.72	<20	15.00	<0.2	0.8	21	675
138684	64	0.2	35.00	1.84	55.0	4.57	318	<0.5	3.41	<20	18.70	0.21	0.7	15	585



NC0054	Depth(m)	Rb	Sb	Sc	Se	Sm	Sr	Ta	Te	Th	U	V	W	Yb	Zn	Zr
138670	30	36.3	8.06	6.80	<5	1.32	3	<1	<5	13.20	<2	398	14.60	1.30	62	59
138671	34	<20	3.53	0.98	<5	0.84	2	<1	<5	0.80	<2	4	36.00	<0.5	31	14
138672	36	<20	4.57	0.94	20.7	0.73	2	<1	<5	1.42	<2	6	89.10	<0.5	22	15
138673	41	<20	2.43	1.82	<5	1.50	2	<1	<5	1.67	<2	6	58.20	0.64	29	34
138674	43	21.7	2.82	4.14	45.9	2.44	6	<1	<5	3.59	<2	49	10.60	1.34	37	80
138675	47	<20	3.13	1.39	<5	1.73	<1	<1	<5	1.70	<2	43	40.30	0.81	677	21
138676	48	44.1	1.69	5.95	<5	2.17	9	1.16	<5	7.62	<2	30	14.80	1.69	47	87
138677	50	<20	14.60	13.30	11.3	2.04	6	<1	<5	2.78	2.42	9	113.00	0.98	119	35
138678	52	<20	7.07	3.64	407.0	1.58	2	<1	<5	3.01	<2	13	87.40	0.82	89	19
138679	54	49.3	1.58	7.16	6.3	3.34	5	1.06	<5	7.15	<2	29	7.05	1.52	771	42
138680	56	69.6	2.64	15.40	<5	4.20	9	1.24	<5	18.10	<2	143	13.20	2.33	91	126
138681	57	<20	3.23	5.64	7.3	1.48	5	1.10	<5	11.30	<2	123	4.41	1.21	85	84
138682	60	82.0	1.49	8.99	<5	2.20	16	1.04	<5	12.00	<2	66	5.99	1.50	48	87
138683	62	47.2	1.36	8.79	<5	2.31	6	<1	<5	11.70	<2	76	18.30	1.24	54	65
138684	64	74.8	1.89	8.94	<5	2.98	14	<1	<5	10.90	<2	71	15.80	1.51	51	78

CA0602	Depth(m)	Al%	Fe%	Mg	Ca	Na%	K%	Ti	Mn	P	S	Ag	As	Au ppb	Ba	Bi	Br
138804	70-72	4.15	10.60	120	65	0.109	<0.2	1630	210	1260	1.21%	3.9	176.00	780.0	121.0	13	<1
138805	72-74	5.85	2.85	1600	70	0.052	1.25	2690	50	150	2.45%	0.6	14.90	1370.0	206.0	22.9	2.21
138806	74-76	5.5	5.10	945	85	0.067	0.65	2290	36	265	4.45%	0.8	58.30	317.0	247.0	17	<1
138807	76-78	3.25	6.76	345	70	0.024	0.51	1420	31	115	7.01%	9.7	163.00	1890.0	121.0	84.7	<1
138808	78-80	2.05	8.39	300	55	0.019	0.41	935	44	88	9.11%	8.4	158.00	4130.0	<100	71.8	<1

CA0602	Depth(m)	Cd	Ce	Co	Cr	Cs	Cu	Eu	Hf	Ir	La	Lu	Mo	Ni	Pb	Rb
138804	70-72	0.2	107.00	16.50	41.9	<1	4480	1.77	3.27	<20	48.00	<0.2	2	21	6340	<20
138805	72-74	<0.1	49.90	20.90	51.4	5.23	3760	1.31	3.98	<20	29.30	0.23	2.5	36	570	115.0
138806	74-76	0.2	54.30	41.60	46.3	2.67	1815	0.83	2.73	<20	27.50	<0.2	1.8	28	1260	52.6
138807	76-78	0.2	25.70	72.30	26.5	1.13	1.16%	0.56	1.60	<20	13.30	<0.2	2.6	19	685	<20
138808	78-80	<0.1	20.20	109.00	21.9	<1	1.85%	<0.5	1.65	<20	11.20	<0.2	3.1	17	545	34.4

CA0602	Depth(m)	Sb	Sc	Se	Sm	Sr	Ta	Te	Th	U	V	W	Yb	Zn	Zr
138804	70-72	2.67	6.62	23.3	5.72	16	<1	<5	7.99	<2	57	81.00	1.11	110	55
138805	72-74	1.63	9.67	6.0	4.49	11	1.05	<5	9.94	<2	49	17.90	1.57	27	79
138806	74-76	2.07	8.67	6.4	3.95	15	1.50	<5	9.45	<2	56	46.50	1.31	30	66
138807	76-78	3.62	4.11	29.6	1.92	6	1.04	<5	5.01	<2	30	146.00	0.55	35	38
138808	78-80	4.63	2.88	28.5	1.65	4	<1	<5	4.03	<2	18	192.00	0.73	25	33

**Appendix 3 Composition of samples, DD97NC0059, New Cobar (ppm, unless indicated otherwise)**

NC0059	Depth(m)	Al%	Fe%	Mg	Ca	Na%	K%	Ti	Mn	P	S	Ag	As	Au ppb	Ba	Bi	Br
138739	5	7	4.93	2750	75	0.039	2.19	2150	225	68	100	<0.1	3.25	<5	361.0	2.7	1.75
138833	49	1.63	25.40	2440	140	0.011	<0.2	940	410	210	6.94%	8.6	67.70	913.0	236.0	51.3	<1
138749	56	2.5	6.66	375	60	0.011	0.33	885	12500	135	125	1.1	4.55	13.5	1230.0	0.9	<1
138751	70	5.5	9.46	3130	110	0.028	1.52	1700	210	150	76	0.3	4.09	<5	254.0	0.2	<1
138752	81	1.97	3.90	365	50	0.012	0.30	850	94	70	40	0.8	17.10	23.2	<100	0.5	<1
138753	82	0.59	1.54	995	<50	<0.01	<0.2	360	120	<30	15	0.4	4.66	<5	<100	<	<1
138754	85	4.55	13.20	6810	105	0.021	0.39	2410	595	80	66	0.7	6.28	22.0	<100	0.9	<1
138755	88	4.8	9.38	580	90	0.016	0.69	1620	115	140	125	1	4.74	76.8	<100	2.5	<1
138756	91	4.7	13.90	1030	100	0.019	0.80	2470	45	135	185	1.1	30.90	23.8	233.0	1.8	<1
138757	95	5.35	13.00	1450	90	0.022	1.22	2540	1860	560	150	2.9	41.40	39.7	304.0	2.5	<1
138758	98	4.2	7.97	825	95	0.014	<0.2	1640	115	68	135	0.7	14.20	106.0	131.0	2	<1
138759	102	5	3.58	1180	75	0.021	0.96	2750	49	100	335	0.6	29.40	50.5	250.0	1.7	<1
138760	105	3.75	9.61	780	85	0.027	0.54	2330	485	320	475	3.3	28.10	60.1	130.0	11.6	1.31
138761	107	3.65	14.70	560	85	0.017	0.32	1940	230	250	645	1.9	65.60	595.0	<100	18.5	<1
138762	110	2.6	8.66	260	95	0.035	<0.2	935	225	72	1860	4	47.40	3550.0	150.0	41.4	<1
138763	112	0.93	13.30	82	105	0.055	<0.2	18	240	405	3080	7.4	369.00	5700.0	<100	73.9	2.86
138764	113	2.5	10.40	260	85	0.018	0.33	1990	46	100	780	2.1	45.60	1440.0	<100	10.2	<1
138765	118	1.65	16.50	90	120	<0.01	<0.2	895	800	120	310	2.6	139.00	1780.0	<100	80.7	1.52
138766	121	3.45	6.06	8350	105	0.014	0.46	1820	695	100	3320	0.2	23.30	64.6	<100	1.4	<1
138767	124	2.35	3.80	4940	70	0.012	0.83	1350	270	130	1.64%	0.8	20.40	46.7	224.0	19.4	<1
138834	127	1.72	11.10	495	940	<0.01	<0.2	405	79	265	2.70%	29.9	490.00	391.0	<100	10.8	1.24
138768	130	0.84	11.60	280	85	<0.01	<0.2	240	57	140	1.18%	4.6	46.80	4780.0	211.0	52.5	<1
138769	134	0.67	15.10	675	55	<0.01	<0.2	170	135	46	1.51%	10.2	33.00	7570.0	<100	84.3	<1

NC0059	Depth(m)	Cd	Ce	Co	Cr	Cs	Cu	Eu	Hf	Ir	La	Lu	Mo	Ni	Pb
138739	5	<0.1	67.80	3.67	63.7	4.97	26	<0.5	3.09	<20	15.40	0.29	0.4	21	24
138833	49	0.8	26.90	112.00	19.1	1.32	4920	0.58	1.55	<20	13.30	<0.2	17.3	16	355
138749	56	0.2	135.00	332.00	19.1	1.74	1675	1.00	1.23	<20	19.90	<0.2	0.7	51	<20
138751	70	0.2	49.50	7.72	58.1	4.73	493	1.25	2.35	<20	28.70	0.33	<0.1	21	<20
138752	81	0.2	19.50	4.73	21.1	1.17	308	<0.5	0.84	<20	9.32	<0.2	0.7	10	<20
138753	82	<0.1	9.23	1.62	12.7	<1	65	<0.5	<0.5	<20	4.30	<0.2	0.7	6	<20
138754	85	0.3	53.00	18.30	51.1	2.81	716	0.75	2.93	<20	25.50	0.29	0.3	19	88
138755	88	0.2	58.70	2.72	55.2	1.19	547	0.88	2.35	<20	21.60	0.24	0.1	17	120
138756	91	0.3	48.50	4.22	55.2	3.16	949	1.30	2.30	<20	27.20	0.26	0.2	19	54
138757	95	0.4	125.00	21.50	54.1	4.77	1580	1.60	2.51	<20	26.90	0.32	0.3	31	1450
138758	98	0.3	38.60	4.11	46.4	1.10	821	1.37	1.76	<20	20.70	0.27	0.1	26	280
138759	102	0.3	35.90	1.62	58.9	3.81	404	0.75	2.41	<20	22.40	0.24	0.6	24	650
138760	105	0.4	68.80	7.93	41.6	2.96	1200	1.42	2.35	<20	28.80	0.23	0.5	9	2060
138761	107	0.6	42.90	3.38	47.3	1.24	1390	1.33	1.96	<20	24.80	0.23	0.7	7	2490
138762	110	0.7	22.10	12.50	30.8	<1	3920	<0.5	0.87	<20	14.00	<0.2	1.9	22	2560
138763	112	0.9	39.90	59.00	9.4	<1	4230	2.67	<0.5	<20	40.90	<0.2	2.7	22	5700
138764	113	0.7	23.30	2.74	41.0	<1	1860	1.01	1.85	<20	13.80	0.21	0.8	20	3160
138765	118	4.3	26.10	120.00	21.3	<1	7840	0.91	1.17	<20	12.10	<0.2	5.7	28	3710
138766	121	5.6	37.70	17.90	41.9	1.59	80	0.56	1.64	<20	20.20	<0.2	0.7	22	350
138767	124	15.6	27.60	25.00	30.0	2.16	533	<0.5	1.50	<20	14.30	<0.2	1.3	15	380
138834	127	5.9	20.70	97.60	20.3	1.34	6.54%	1.75	0.58	<20	17.90	0.65	3.8	22	3370
138768	130	1.2	8.02	51.40	8.4	<1	1550	<0.5	1.09	<20	3.23	<0.2	13	8	670
138769	134	0.6	5.75	51.40	6.9	<1	8240	<0.5	<0.5	<20	3.04	<0.2	23.2	8	74

NC0059	Depth(m)	Rb	Sb	Sc	Se	Sm	Sr	Ta	Te	Th	U	V	W	Yb	Zn	Zr
138739	5	176.0	0.48	13.80	<5	3.17	10	1.57	<5	14.20	2.14	64	8.13	2.01	133	69
138833	49	<20	10.60	2.57	58.2	2.15	18	<1	<5	3.13	<2	25	948.00	0.86	239	31
138749	56	38.5	2.37	3.98	<5	5.88	4	<1	<5	3.44	<2	34	13.40	1.28	122	24
138751	70	114.0	1.19	10.30	<5	6.10	13	<1	<5	11.30	2.53	56	6.36	2.15	115	60
138752	81	25.6	2.38	3.00	<5	1.98	4	<1	<5	3.53	<2	20	13.40	0.74	62	22
138753	82	<20	0.97	0.87	<5	0.80	2	<1	<5	1.41	<2	6	12.50	<0.5	15	8
138754	85	69.2	2.26	8.58	<5	5.26	9	<1	<5	10.70	<2	54	10.40	2.02	101	66
138755	88	32.4	1.51	8.87	<5	4.44	12	<1	<5	9.82	3.36	66	5.54	1.66	66	53
138756	91	71.0	1.27	8.97	<5	4.85	20	<1	<5	9.23	<2	63	3.89	1.72	75	63
138757	95	106.0	2.32	14.50	<5	4.62	10	<1	<5	10.20	7.74	131	328.00	2.17	349	63
138758	98	<20	1.69	5.92	<5	5.08	6	<1	<5	7.62	3.74	44	7.51	1.85	41	47
138759	102	78.9	3.25	10.20	<5	3.61	9	<1	<5	11.00	2.93	98	37.60	1.65	50	66
138760	105	58.3	3.71	7.61	<5	4.76	7	<1	<5	10.00	<2	60	57.80	1.62	87	58
138761	107	30.3	3.04	7.61	<5	4.58	8	<1	<5	8.90	4.02	84	44.80	1.57	112	49
138762	110	<20	3.74	2.73	7.6	2.94	6	<1	<5	4.13	5.23	97	47.10	0.96	200	25
138763	112	<20	2.65	3.44	36.4	11.10	10	<1	<5	<0.5	13.40	16	38.10	1.12	954	<5
138764	113	21.5	4.95	4.19	<5	2.84	5	<1	<5	6.69	3.42	51	50.20	1.40	90	49
138765	118	<20	4.46	4.65	8.2	3.09	7	<1	<5	3.25	3.25	22	113.00	1.07	2070	25
138766	121	35.3	1.07	6.05	<5	3.01	15	<1	<5	7.41	<2	42	20.60	1.12	253	47
138767	124	48.5	2.96	4.57	<5	2.43	11	<1	<5	5.92	<2	30	26.10	0.74	224	35
138834	127	<20	1.31	1.79	84.3	5.71	21	<1	<5	2.15	3.09	14	122.00	4.13	667	12
138768	130	<20	9.59	1.84	6.9	0.64	5	<1	<5	1.07	<2	19	1200.00	<0.5	153	10
138769	134	<20	8.66	0.84	10.5	0.50	4	<1	<5	<0.5	2.02	18	230.00	<0.5	111	7

**Appendix 4 Composition of samples, DD97NC0060, New Cobar (ppm, unless indicated otherwise)**

NC0060	Depth(m)	Al%	Fe%	Mg	Ca	Na%	K%	Ti	Mn	P	S	Ag	As	Au ppb	Ba	Bi	Br
138691	5	6.7	9.62	1160	60	0.035	0.99	2760	68	215	190	0.2	16.30	8.4	288.0	2.5	2.53
138705	86	9.45	2.25	4050	75	0.041	3.01	4010	49	140	1.85%	0.2	82.70	14.5	469.0	10.9	<1
138706	88	9.5	3.33	9170	95	0.046	3.48	4670	255	155	1.23%	0.2	11.70	7.3	608.0	4.2	<1
138708	93	10.2	1.81	4010	<50	0.033	2.74	4040	49	96	6830	0.4	29.50	11.6	316.0	5.1	<1
138710	99	7.9	0.99	1130	85	0.057	0.95	2970	37	190	1900	0.5	26.50	3060.0	227.0	3.3	<1
138711	102	7.3	5.01	890	100	0.021	0.57	2250	3920	505	505	1.5	20.60	20.8	245.0	9.4	<1
138712	104	3.25	6.76	200	105	0.017	<0.2	900	3970	100	385	2.3	238.00	406.0	<100	27.2	1.02
138713	105	6.8	0.37	515	110	0.024	0.28	2510	215	105	235	1.2	7.61	33.6	113.0	4.1	<1
138714	108	3.5	6.63	195	105	0.013	<0.2	975	410	76	175	4	21.20	214.0	<100	2.1	<1
138715	110	4.45	6.64	115	215	0.011	<0.2	1140	13	70	9.17%	2	291.00	279.0	<200	28	<1
138716	112	3.95	11.90	1650	75	0.011	0.31	1820	155	92	1.42%	0.2	55.20	129.0	<100	6.4	<1
138717	114	3	14.80	520	70	0.010	<0.2	1030	64	62	7.43%	1.2	453.00	1170.0	<100	33.6	1.88
138718	115	1.65	11.10	105	120	0.013	<0.2	405	23	70	5.75%	10	234.00	3180.0	<100	66.4	<1
138719	118	2.7	12.50	780	85	0.010	<0.2	1090	79	78	5.11%	3.3	120.00	2100.0	112.0	39.8	<1
138720	120	3.8	9.02	6180	60	<0.01	<0.2	1800	605	60	3.20%	1.3	89.80	409.0	116.0	12.8	<1
138721	123	1.72	2.99	76	65	<0.01	<0.2	<10	28	40	3.85%	113	20.10	75200.0	<200	759	<1
138722	125	1.23	1.87	1950	60	<0.01	<0.2	190	205	<30	2390	0.9	9.35	59.1	<100	9.2	<1
138723	128	0.97	14.20	1870	<50	<0.01	<0.2	390	195	54	14.10%	8.4	660.00	1730.0	<100	116	1.82
138724	130	1.8	7.08	3600	70	0.011	<0.2	860	445	60	3.50%	3.7	60.80	284.0	<100	17.3	<1
138725	132	4.8	9.91	11400	95	0.012	0.64	2360	910	96	1.83%	0.2	6.63	<5	137.0	3.9	1.28
138726	134	2.75	5.17	7260	60	0.011	0.35	1470	625	36	6090	3.3	1.70	<5	<100	1.3	<1
138831	138	1.46	7.84	3740	85	<0.01	<0.2	330	280	46	6.82%	18.8	117.00	18500.0	<100	411	<1
138727	140	1	11.60	2440	80	<0.01	<0.2	215	175	58	11.12%	12.4	136.00	3270.0	<100	97.4	<1
138728	142	3.4	9.19	7440	70	0.014	0.69	1750	590	78	4.80%	1.3	204.00	233.0	225.0	13.4	<1
138729	144	4.85	8.09	9610	290	0.020	1.21	2460	850	220	2.20%	0.2	16.00	15.7	210.0	7.3	<1
138730	146	4.6	11.50	9190	110	0.017	1.00	2280	765	125	6.25%	5.1	322.00	617.0	313.0	12.7	1.12
138731	147	2.45	13.00	5080	75	<0.01	<0.2	1300	515	86	12.21%	57.7	439.00	771.0	<100	73.7	<1
138732	148	1.79	11.60	4040	85	<0.01	<0.2	785	420	48	8.85%	19.4	79.50	1090.0	<100	9.6	<1
138733	150	3.75	8.80	8880	85	0.012	0.29	2680	1000	88	4920	0.6	2.58	31.3	<100	0.4	<1
138832	152	0.9	4.61	2760	90	0.011	<0.2	415	340	36	3.05%	15.5	1.95	11500.0	<100	96.9	<1
138734	154	2.45	7.09	8940	90	0.015	<0.2	1560	625	94	3.55%	2.5	3.32	331.0	148.0	14.7	<1
138735	157	3.95	7.60	10500	90	0.015	0.53	2470	1050	72	2290	0.3	1.03	19.5	150.0	0.9	<1
138736	158	3.95	8.97	24500	100	<0.01	<0.2	1290	1170	96	1.02%	2.2	<1	278.0	<100	142	<1

NC0060	Depth(m)	Cd	Ce	Co	Cr	Cs	Cu	Eu	Hf	Ir	La	Lu	Mo	Ni	Pb
138691	5	1.6	26.50	2.57	57.7	2.40	131	<0.5	3.55	<20	10.20	0.23	0.5	19	58
138705	86	0.1	74.00	24.10	82.5	8.02	412	1.15	3.73	<20	41.80	0.38	0.8	42	190
138706	88	0.3	106.00	27.20	91.0	9.81	2590	1.94	4.69	<20	61.80	0.54	0.7	29	270
138708	93	0.2	70.70	8.43	88.6	7.86	3480	1.09	3.94	<20	39.70	0.39	0.9	42	455
138710	99	0.2	33.10	1.22	61.4	2.88	265	0.59	3.03	<20	21.60	0.24	1.4	12	1110
138711	102	0.6	59.20	74.10	48.7	2.45	2310	0.67	2.16	<20	25.40	0.21	2.1	11	4750
138712	104	1.4	184.00	118.00	29.1	<1	3830	0.80	0.88	<20	12.70	<0.2	8.7	12	3550
138713	105	0.4	25.50	10.10	51.9	1.29	513	0.51	2.73	<20	16.20	0.20	0.6	9	440
138714	108	0.8	21.20	16.50	27.7	<1	671	0.53	1.16	<20	13.10	<0.2	2	11	760
138715	110	0.4	26.10	74.90	20.0	<1	26.94%	<0.5	1.15	<20	10.70	<0.2	6.1	30	375
138716	112	0.2	50.30	26.80	42.0	1.61	191	0.90	1.94	<20	24.90	<0.2	0.9	18	32
138717	114	6.5	23.60	101.00	24.6	<1	454	0.54	1.12	<20	11.90	<0.2	2	12	175
138718	115	7.4	21.10	128.00	12.3	<1	9710	<0.5	<0.5	<20	9.89	<0.2	7.2	10	385
138719	118	1.7	36.80	115.00	26.5	<1	2900	0.70	1.08	<20	17.40	<0.2	4.8	16	115
138720	120	1	37.60	58.30	35.6	<1	932	0.76	1.96	<20	19.80	<0.2	2	18	170
138721	123	0.4	<4	107.00	<10	<1	1.28%	<0.5	<0.5	<20	1.12	<0.2	7.3	25	5230
138722	125	0.6	5.06	5.52	8.6	<1	1975	<0.5	<0.5	<20	2.53	<0.2	1.1	6	445
138723	128	0.3	9.08	199.00	11.8	<1	3660	<0.5	0.73	<20	4.78	<0.2	1.7	8	465
138724	130	3.5	26.20	35.80	18.6	1.01	1835	<0.5	1.12	<20	12.90	<0.2	3.2	11	325
138725	132	1.2	57.20	25.40	52.9	2.05	168	0.97	2.61	<20	27.10	0.24	0.8	25	<20
138726	134	1.8	27.40	21.30	32.5	1.51	216	0.52	1.87	<20	11.50	<0.2	0.7	16	270
138831	138	8.3	8.67	89.40	8.4	<1	2.25%	<0.5	0.81	<20	4.79	<0.2	2.5	18	490
138727	140	3	11.80	187.00	<5	1.25	2.25%	<0.5	<0.5	<20	5.25	<0.2	4.7	32	190
138728	142	0.4	39.30	149.00	38.4	2.35	906	0.71	1.64	<20	19.30	<0.2	1.1	21	125
138729	144	<0.1	53.10	45.20	52.8	5.30	23	0.72	2.12	<20	25.00	0.23	0.6	40	26
138730	146	0.2	46.90	75.80	51.2	3.82	1.06%	0.79	1.80	<20	23.20	0.22	0.8	23	52
138731	147	67.3	23.70	113.00	30.0	2.01	7360	<0.5	1.19	<20	12.80	<0.2	4.4	49	18.50%
138732	148	7	17.60	80.60	19.6	1.03	4.60%	<0.5	0.78	<20	8.67	<0.2	1.2	18	225
138733	150	0.3	61.50	28.90	70.7	1.64	1025	0.79	5.87	<20	28.40	0.30	0.7	24	28
138832	152	3.7	7.81	21.80	19.3	<1	2.70%	<0.5	0.69	<20	4.23	<0.2	1.7	17	115
138734	154	12.9	33.60	58.00	43.7	<1	2840	<0.5	3.14	<20	15.50	<0.2	2.2	16	94
138735	157	0.1	50.80	16.70	56.3	1.88	99	0.89	4.06	<20	23.90	0.24	0.5	20	66
138736	158	0.4	38.90	24.00	29.6	<1	251	0.86	1.72	<20	20.00	<0.2	29.6	16	285

NC0060	Depth(m)	Rb	Sb	Sc	Se	Sm	Sr	Ta	Te	Th	U	V	W	Yb	Zn	Zr
138691	5	64.8	1.31	13.80	<5	1.65	24	<1	<5	12.50	<2	68	10.20	1.41	156	91
138705	86	213.0	1.92	14.60	<5	6.07	17	2.33	<5	15.40	2.43	91	9.19	2.56	34	107
138706	88	252.0	1.39	15.60	<5	9.41	20	<1	<5	18.50	2.44	113	7.68	3.28	154	127
138708	93	215.0	1.74	16.50	<5	5.42	13	<1	<5	16.60	3.24	106	9.61	2.44	35	106
138710	99	60.4	2.21	10.60	<5	2.58	18	<1	<5	13.70	2.55	63	48.50	1.59	125	78
138711	102	50.2	2.52	11.40	<5	3.46	14	<1	<5	11.70	6.40	94	45.60	1.44	121	58
138712	104	<20	5.71	7.00	6.7	3.47	10	<1	<5	6.36	12.90	39	63.90	1.07	166	27
138713	105	<20	1.54	8.80	<5	2.18	14	1.41	<5	11.90	2.86	57	25.70	1.37	179	64
138714	108	<20	2.06	3.76	69.8	1.72	7	<1	<5	5.69	2.36	26	16.20	0.56	105	27
138715	110	<20	6.92	4.83	94.1	1.38	5	<1	<20	5.93	<2	48	14.30	0.56	171	31
138716	112	25.5	3.14	9.57	<5	3.31	14	1.54	<5	8.22	<2	97	15.20	1.20	141	48
138717	114	<20	8.95	6.94	11.9	1.63	5	<1	<5	4.61	<2	68	26.70	<0.5	134	27
138718	115	<20	4.98	4.98	49.9	1.43	9	<1	<5	2.24	2.27	20	47.10	<0.5	154	12
138719	118	<20	4.00	7.60	32.4	2.79	9	<1	<5	4.80	<2	41	48.10	0.52	159	29
138720	120	<20	1.82	7.16	7.3	3.03	4	<1	<5	7.39	<2	45	49.90	0.96	158	47
138721	123	<20	1.83	0.87	35.6	<0.5	11	<1	<5	<0.5	<2	12	13.40	<0.5	413	<5
138722	125	<20	1.03	1.29	<5	0.37	<1	<1	<5	0.80	<2	11	34.30	<0.5	190	5
138723	128	<20	4.84	1.45	53.3	0.81	<1	<1	<5	0.97	<2	11	524.00	<0.5	138	11
138724	130	<20	2.03	2.84	13.7	2.22	4	<1	<5	3.67	<2	20	25.00	0.57	1240	24
138725	132	55.5	1.26	8.52	<5	4.90	10	<1	<5	9.36	<2	59	18.50	1.65	597	63
138726	134	27.1	1.63	4.82	<5	2.39	4	<1	<5	6.26	<2	35	27.50	1.01	333	45
138831	138	<20	5.02	1.78	41.4	0.85	3	<1	<5	0.60	<2	17	356.00	<0.5	234	11
138727	140	<20	6.96	1.21	45.8	1.08	2	<1	<5	<0.5	<2	10	801.00	<0.5	301	6
138728	142	55.7	4.09	5.91	10.1	3.23	10	<1	<5	6.63	<2	42	28.00	1.11	346	48
138729	144	118.0	1.49	8.67	<5	4.10	42	<1	<5	10.30	<2	59	8.53	1.65	262	63
138730	146	85.1	1.75	7.85	17.5	3.62	16	<1	<5	9.61	<2	55	7.98	1.47	626	59
138731	147	<20	50.40	4.40	61.6	1.35	3	<1	<5	5.77	<2	33	22.50	1.09	3.65%	37
138732	148	<20	4.34	3.36	31.8	1.44	2	<1	<5	2.67	<2	30	53.80	0.57	1.02%	21
138733	150	31.5	0.82	7.39	<5	5.22	11	<1	<5	11.10	2.57	50	20.50	2.07	775	99
138832	152	<20	2.37	1.44	<5	0.70	4	<1	<5	0.81	<2	15	42.90	<0.5	2330	15
138734	154	26.9	1.52	4.54	10.3	2.86	11	<1	<5	6.27	<2	38	51.40	1.23	3380	57
138735	157	40.8	0.54	7.19	<5	4.08	16	1.09	<5	9.53	<2	50	9.55	1.77	456	79
138736	158	<20	2.97	5.74	8.2	3.77	20	<1	<5	5.10	2.35	55	16.10	1.14	311	41

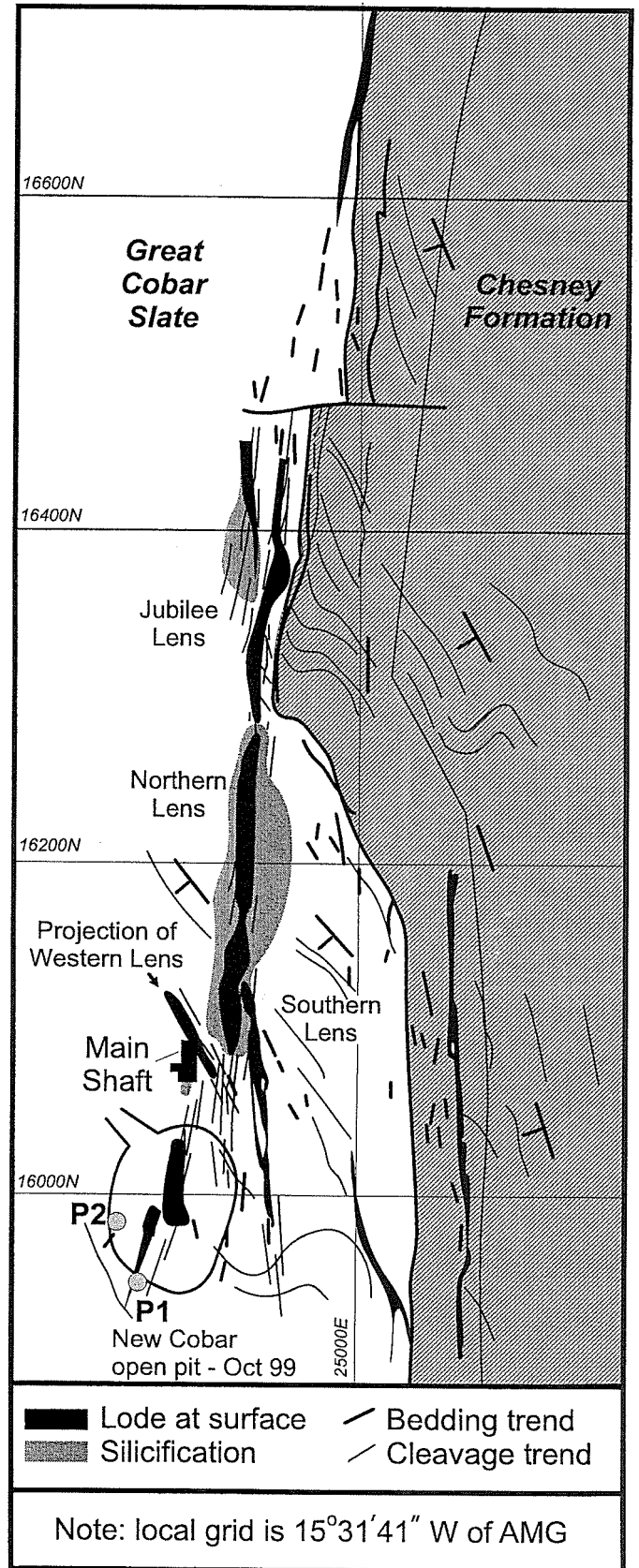
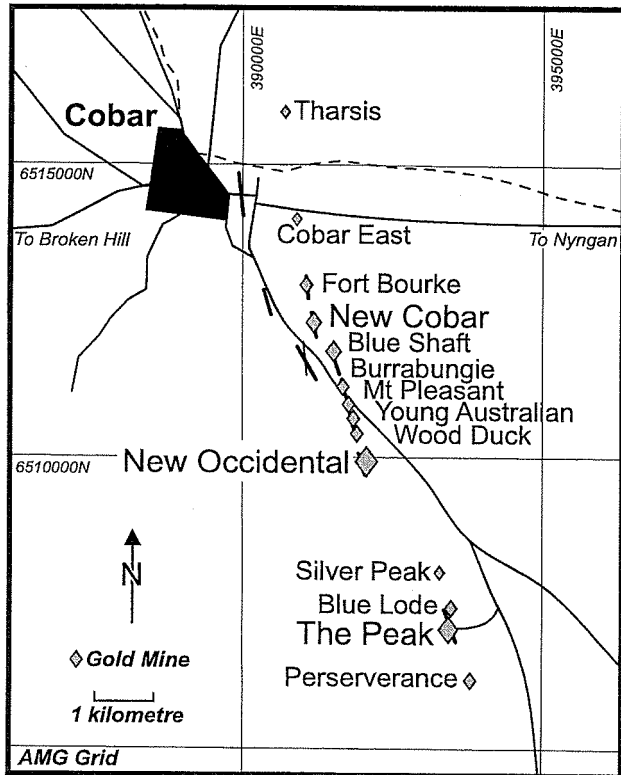


Figure 1. The location of the New Cobar Deposit in the Cobar Gold Field (after Stegman and Pocock, 1996; Leah and Roberts, 2000)



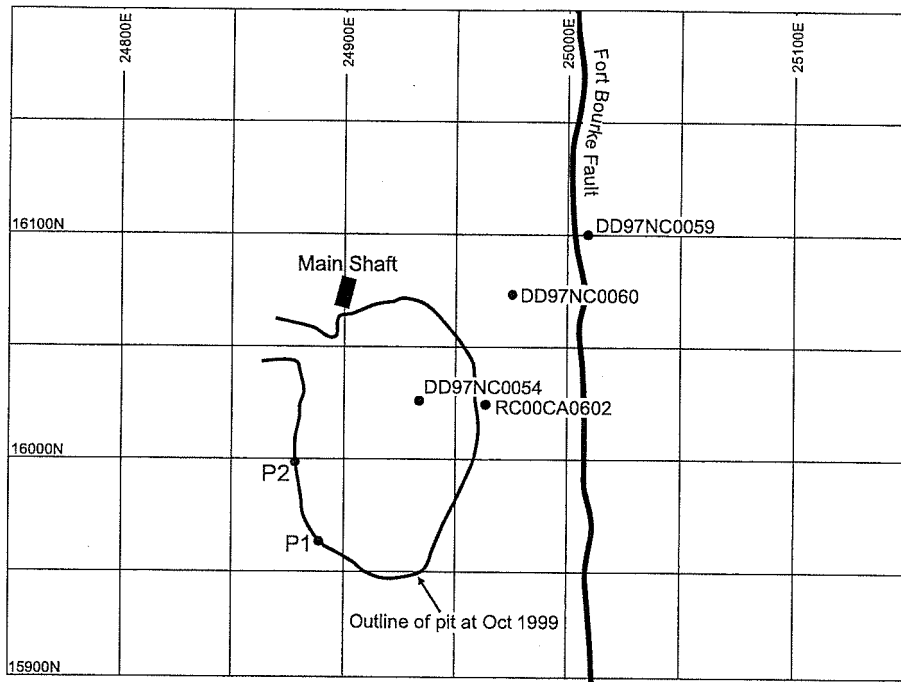


Figure 2. Location of drill holes and profiles at the New Cobar South open pit

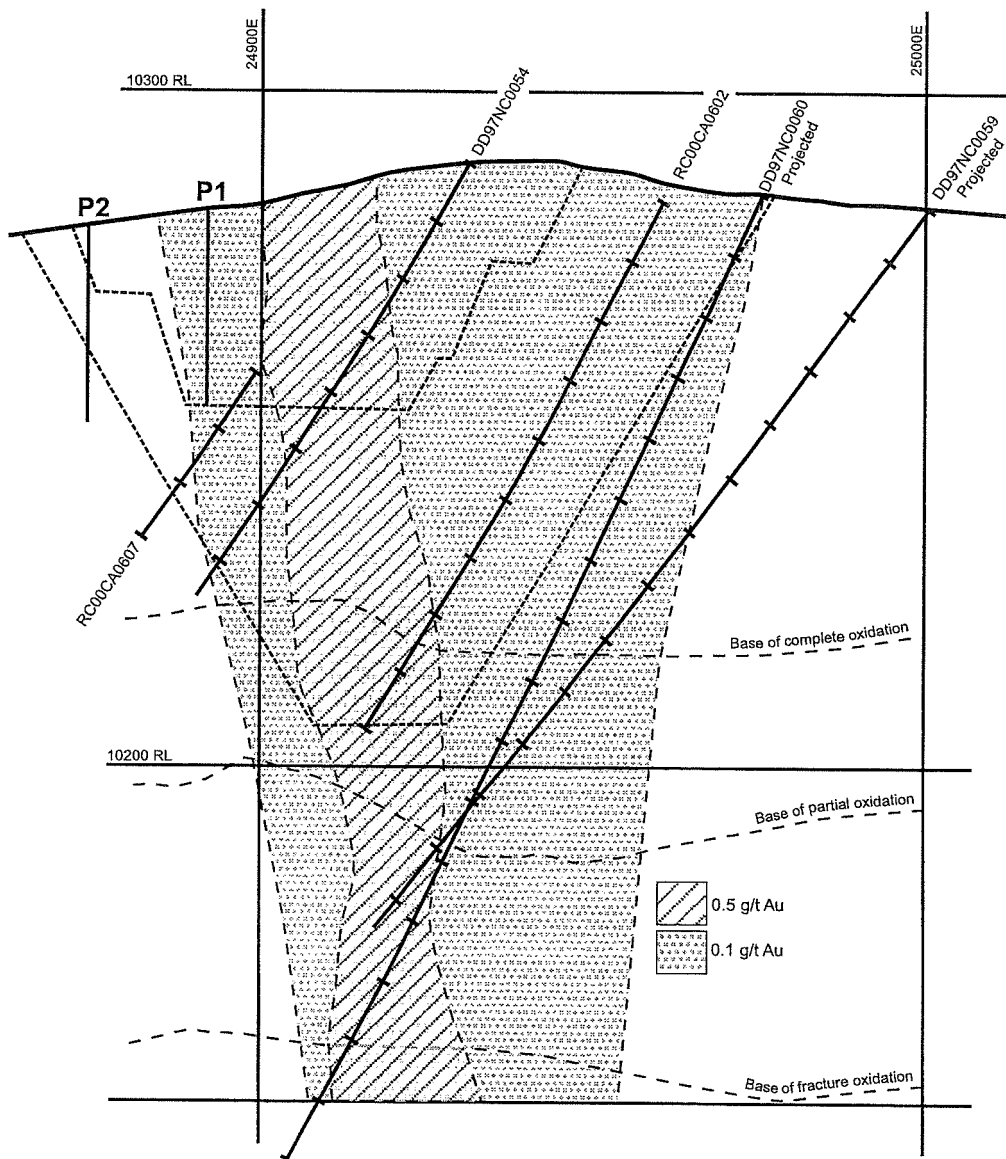


Figure 3. Section at 16025N, New Cobar (after Peak Gold Mines Pty Ltd)

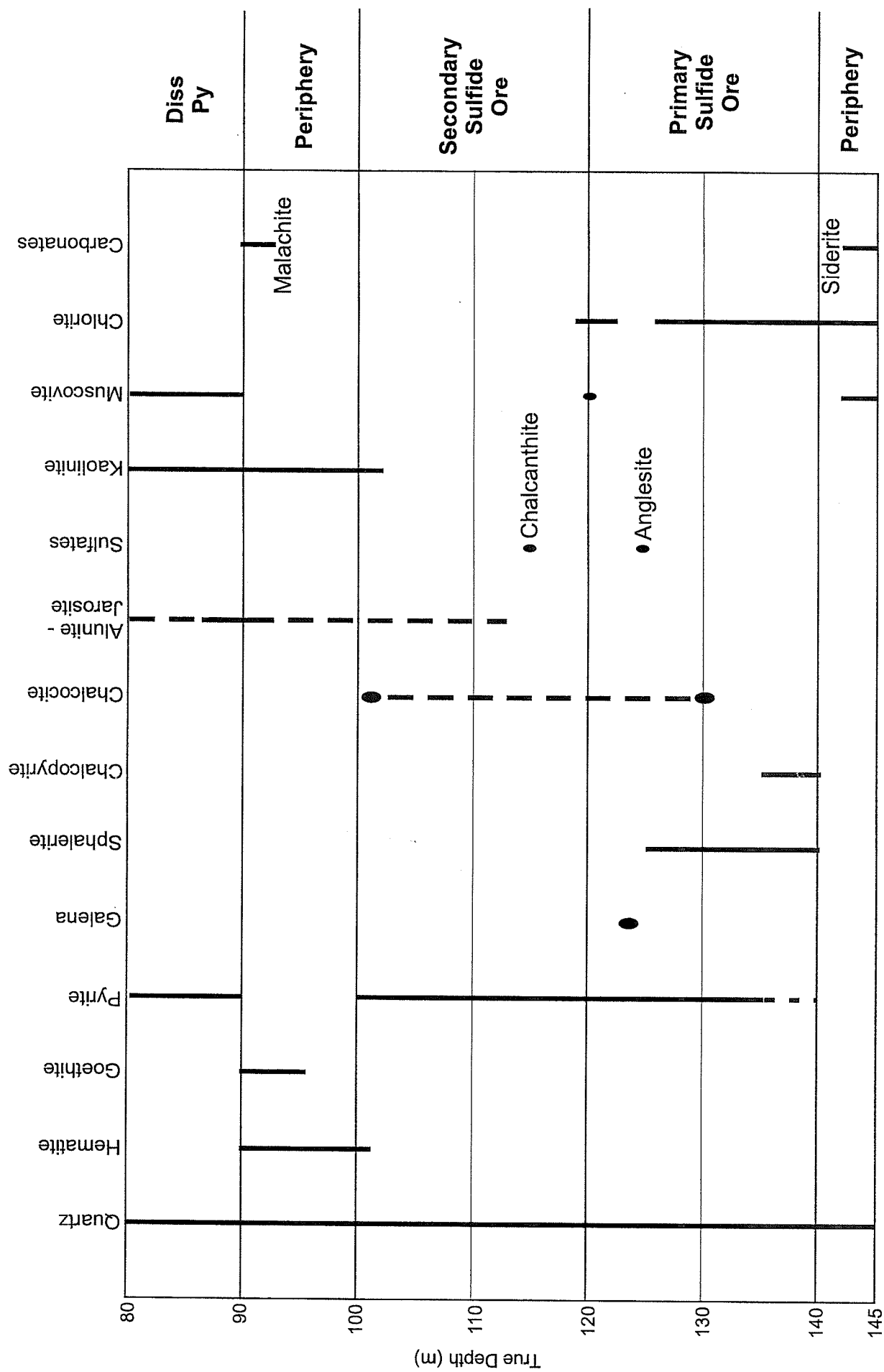


Figure 4. Mineralogical variation below the base of complete oxidation in DD97NC0060, New Cobar (determined by X-ray diffraction).

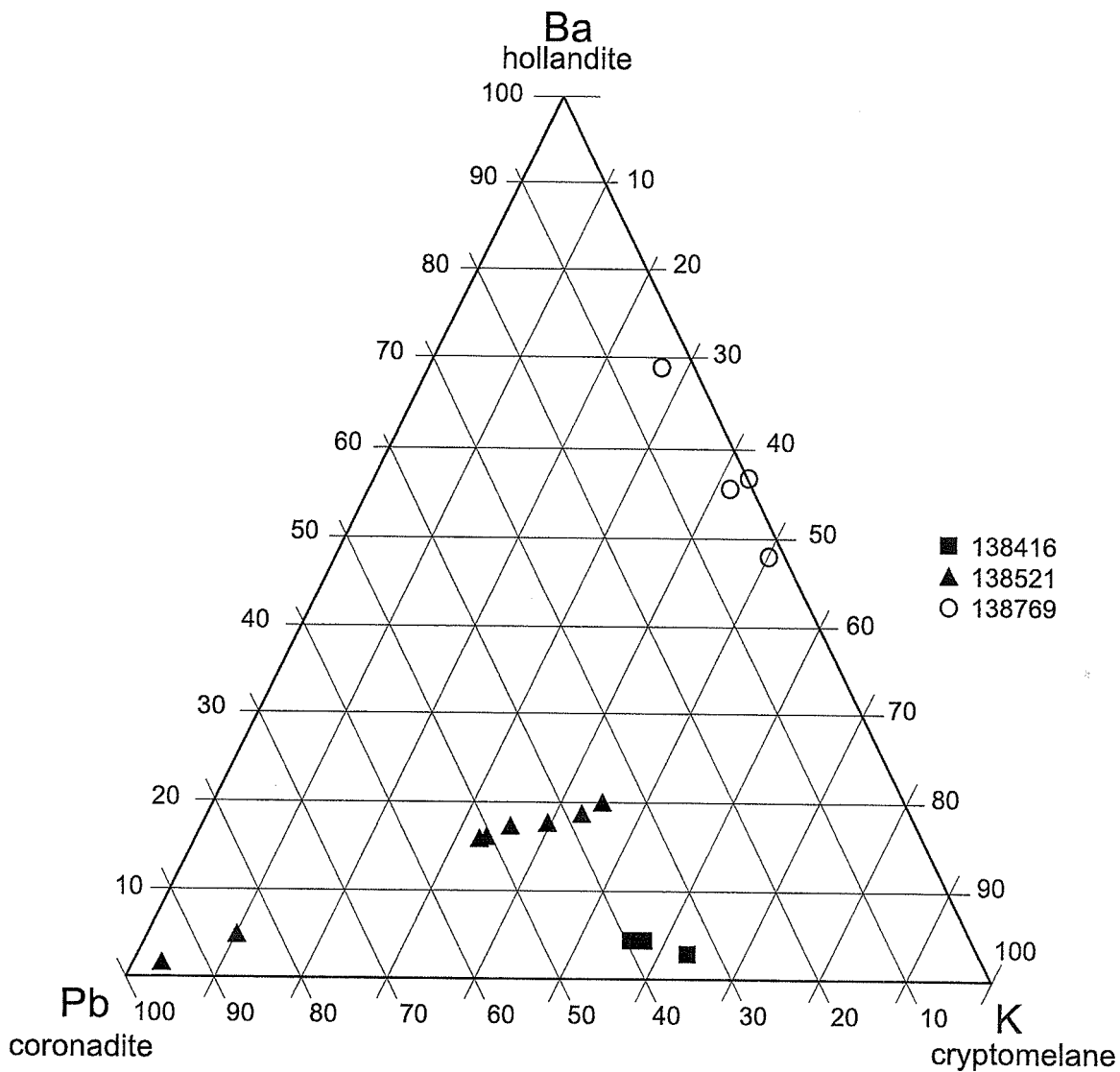


Figure 5. Compositional variations in cryptomelane-hollandite-coronadite series minerals, New Cobar

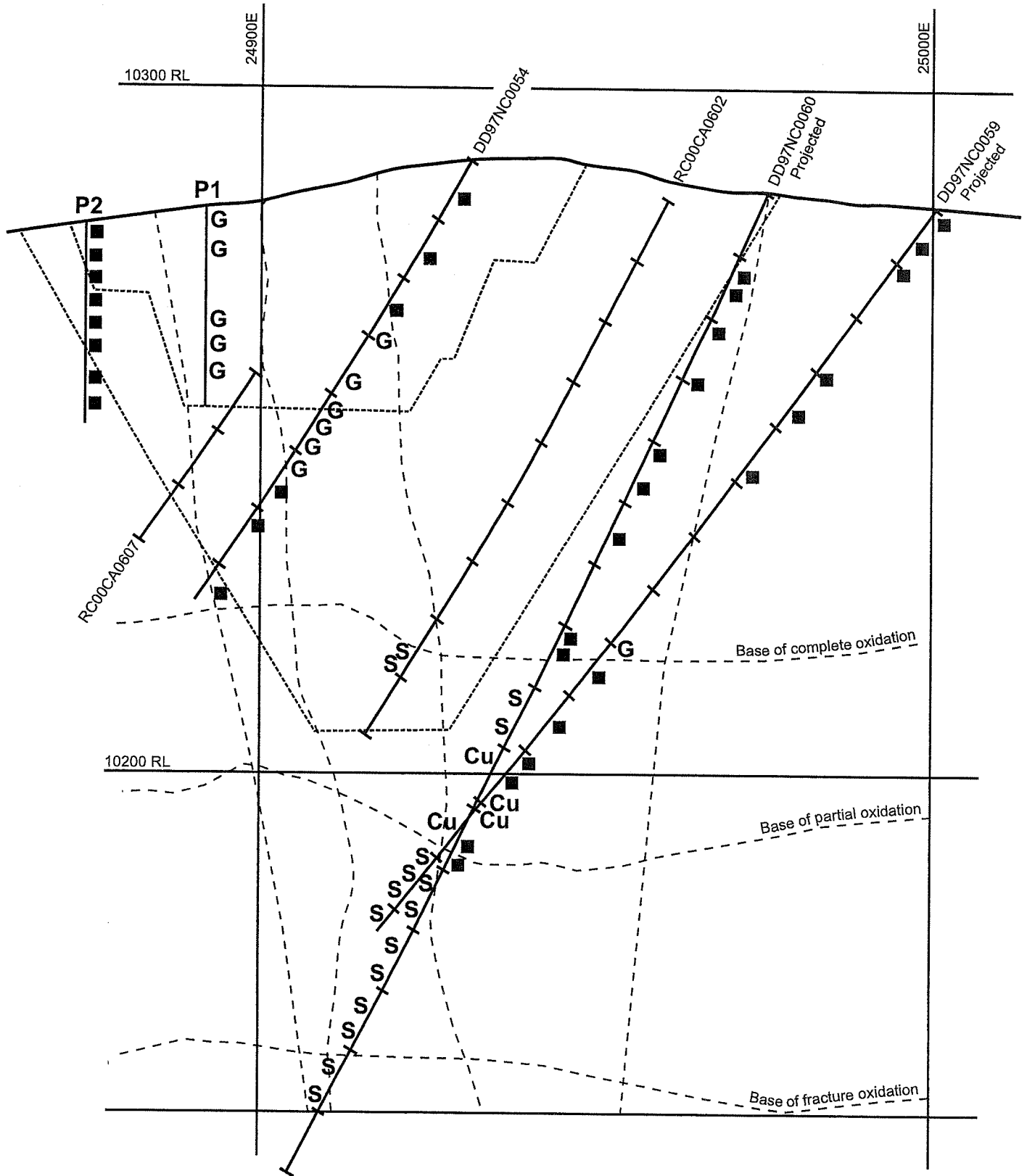


Figure 6. Section at 16025N, New Cobar, showing distribution of sulfides, pyrite casts and gossanous features

- |          |                    |           |                         |
|----------|--------------------|-----------|-------------------------|
| <b>S</b> | Sulfides           | <b>Cu</b> | Cu staining / malachite |
| <b>■</b> | Casts after pyrite | <b>G</b>  | Gossanous               |

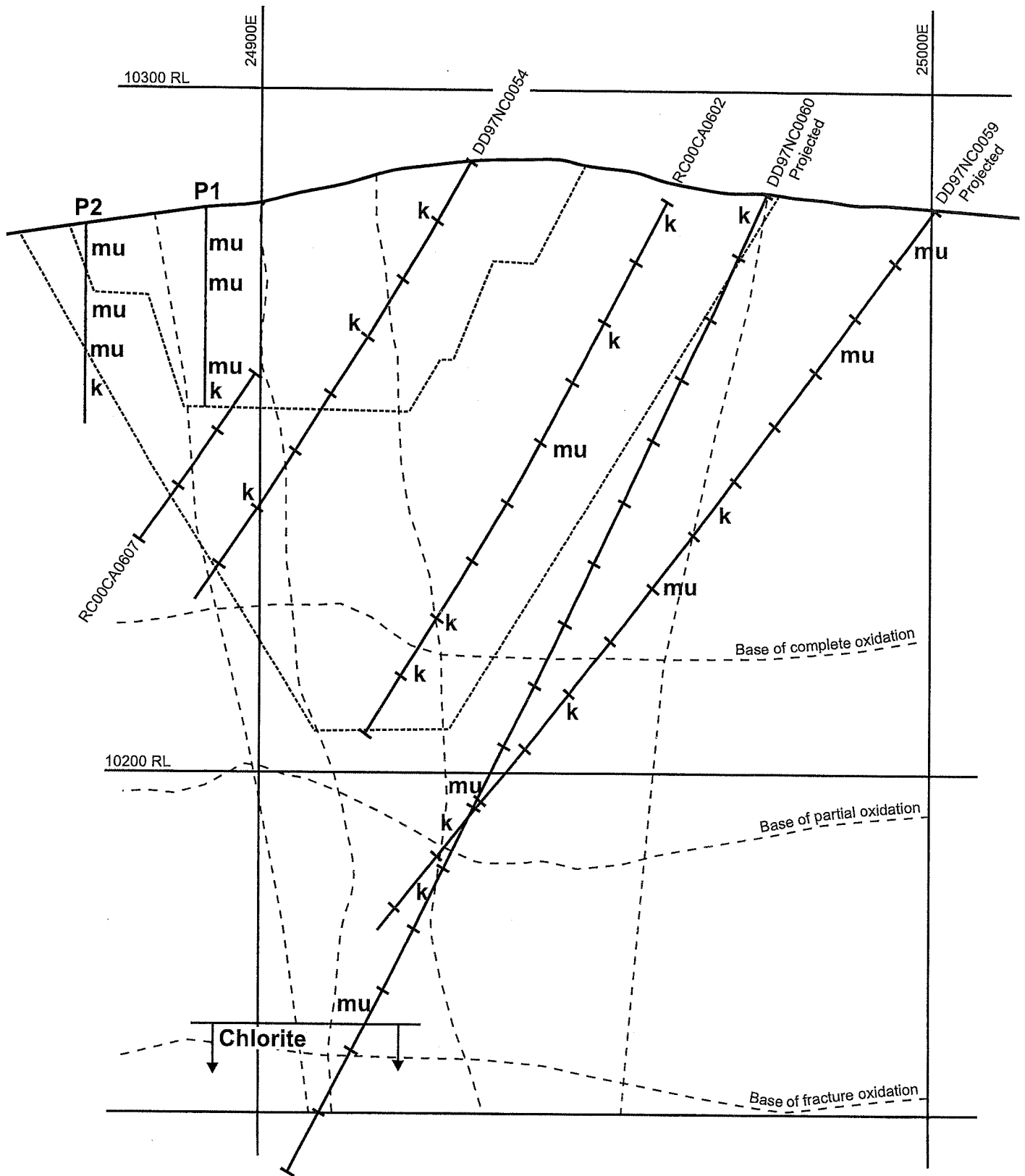


Figure 7. Section at 16025N, New Cobar, showing distribution of dominant kaolinite (k) and muscovite (mu).

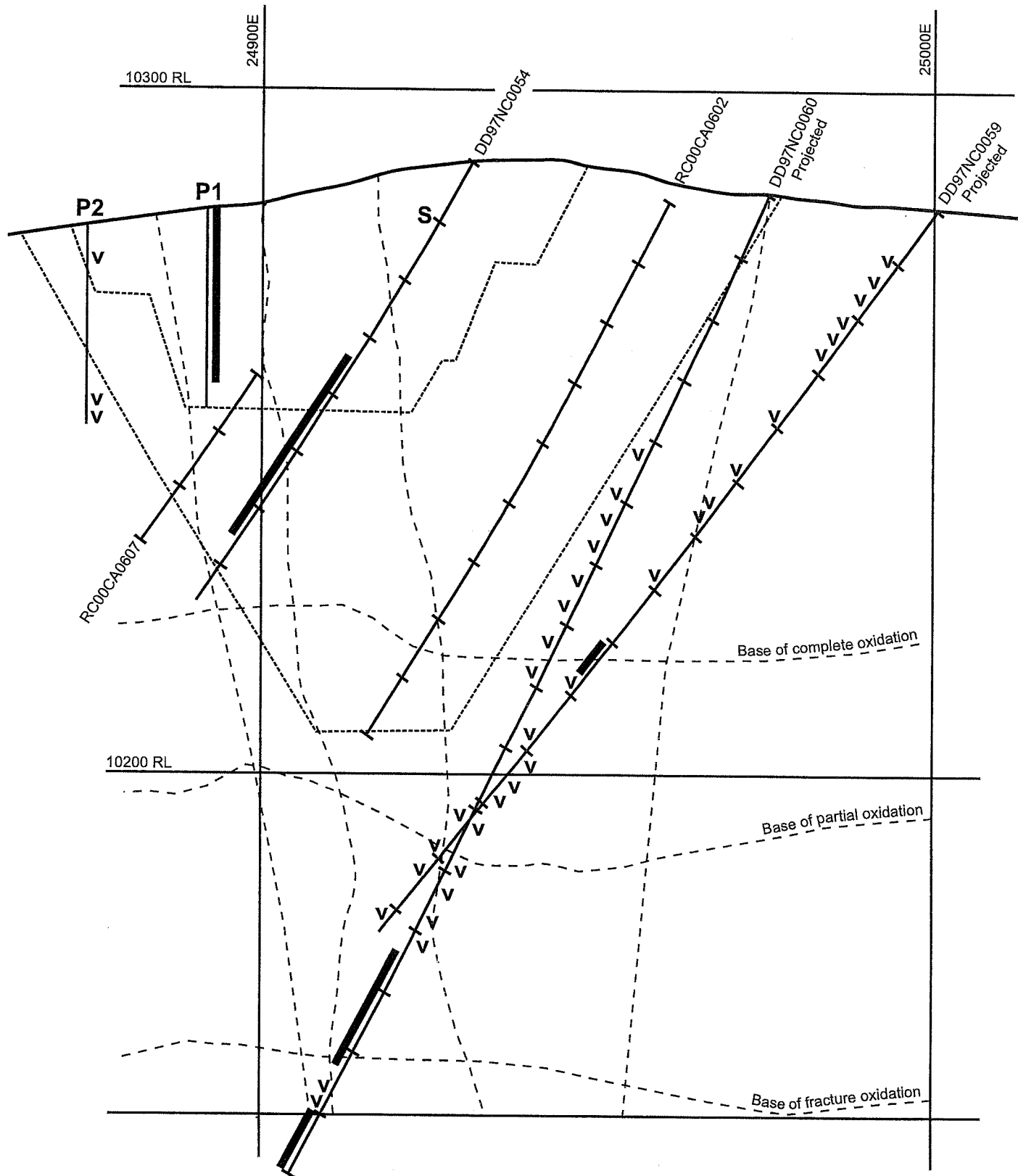



Figure 8. Section at 16025N, New Cobar, showing distribution of zones of silicification and abundant quartz veining

S or  Silicification    v Veining

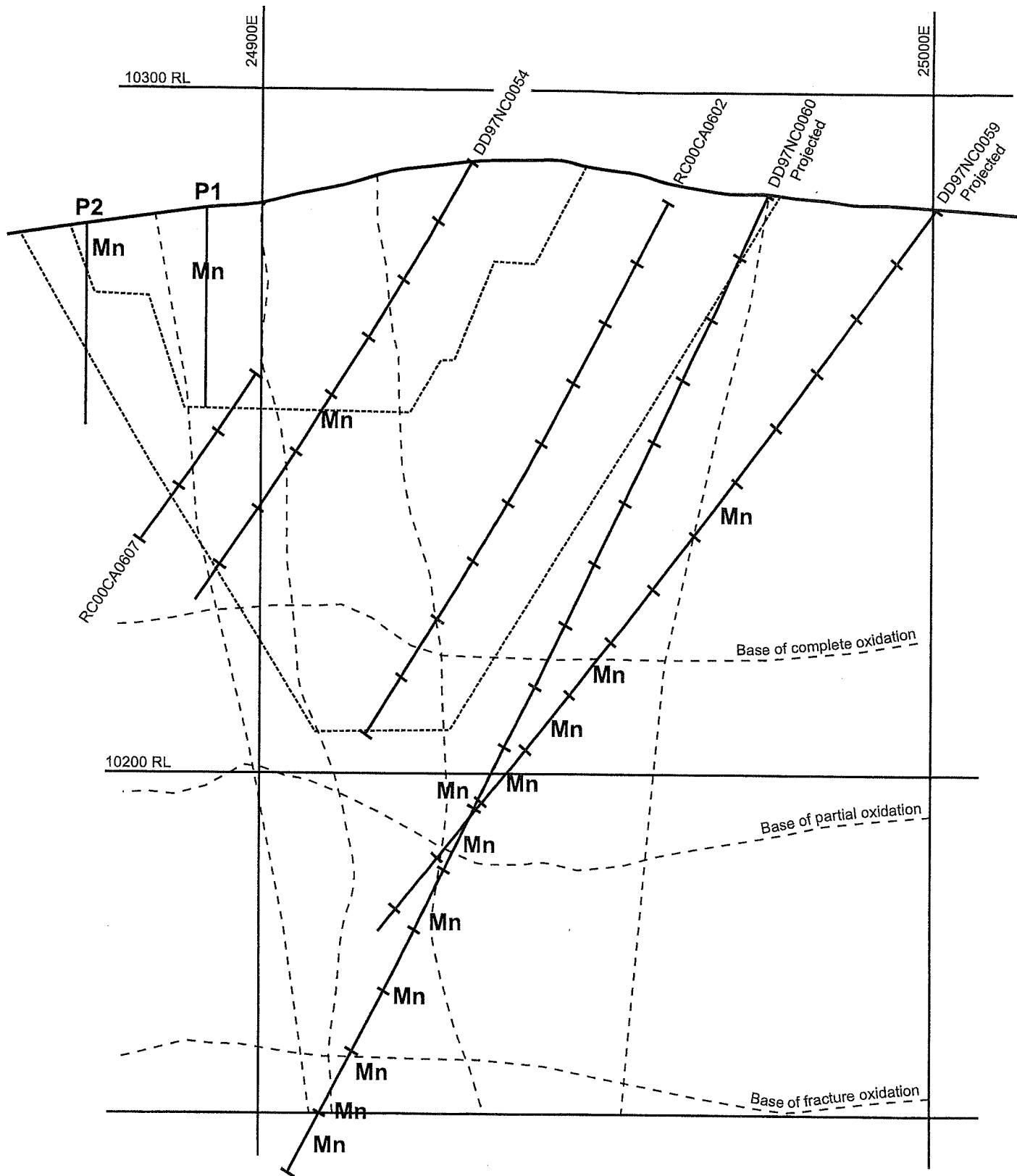
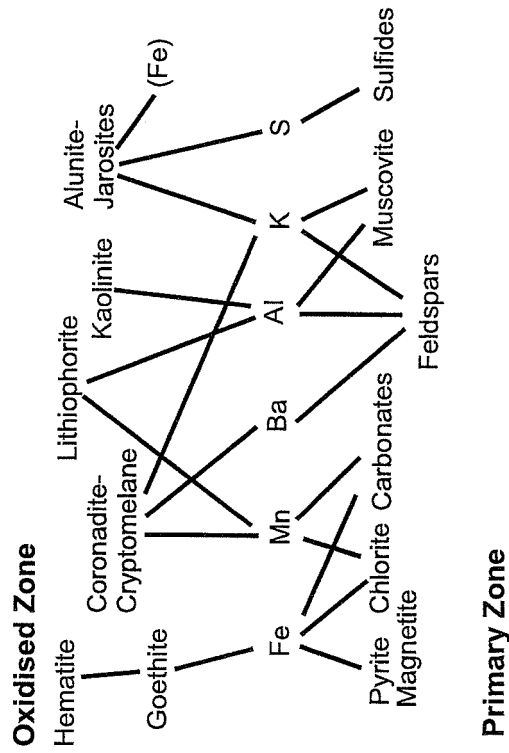


Figure 9. Section at 16025N, New Cobar, showing distribution of abundant Mn (Mn >500 ppm).

### Major Element Distribution



### Significant Minor Element Distribution

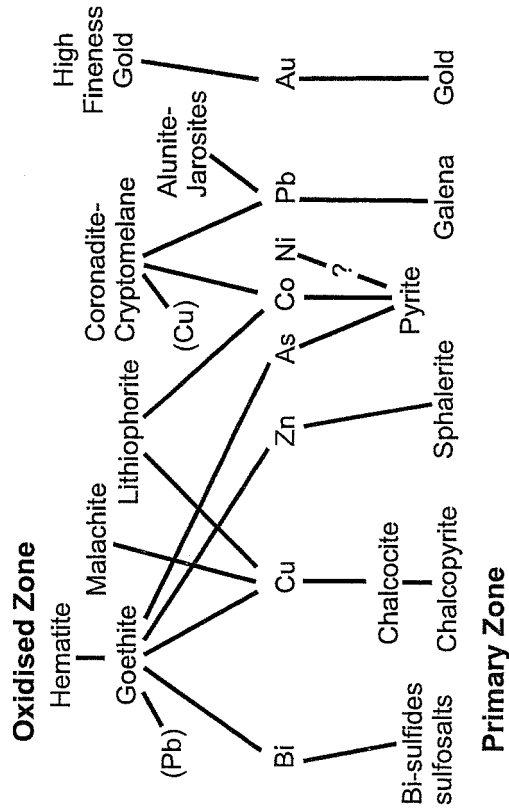


Figure 10. Schematic summary of some major and minor element hosts in the primary and oxidised zones, New Cobar.



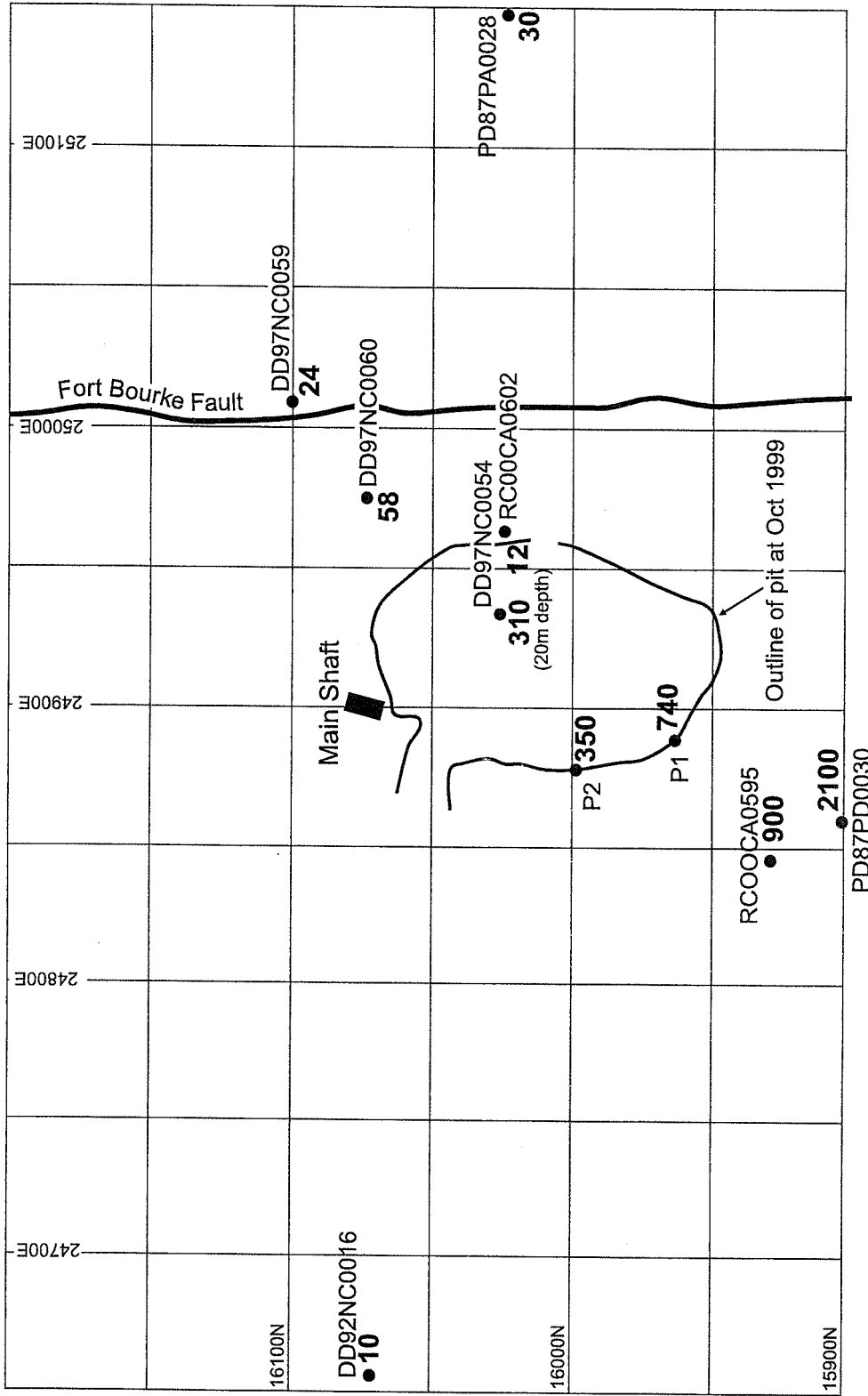


Figure 11. Location of drill holes and profiles at New Cobar South Open Pit, showing Pb content (ppm) in near surface samples.